The Cell Surface 11 (2024) 100124

Contents lists available at ScienceDirect

The Cell Surface

journal homepage: www.sciencedirect.com/journal/the-cell-surface

Leucine rich repeat-malectin receptor kinases IGP1/CORK1, IGP3 and IGP4 are required for arabidopsis immune responses triggered by β-1,4-D-Xylo-oligosaccharides from plant cell walls

Patricia Fernández-Calvo [a,1,*], Gemma López [a], Marina Martín-Dacal [a,b], Meriem Aitouguinane [a], Cristian Carrasco-López [a], Sara González-Bodí [a], Laura Bacete [a,b,2], Hugo Mélida [a,3], Andrea Sánchez-Vallet [b], Antonio Molina [a,b,*]

[a] Centro de Biotecnología y Genómica de Plantas, Universidad Politécnica de Madrid (UPM), Instituto Nacional de Investigación y Tecnología Agraria y Alimentaria (INIA/CSIC), Campus de Montegancedo UPM, Pozuelo de Alarcón, Madrid, Spain
[b] Departamento de Biotecnología-Biología Vegetal, Escuela Técnica Superior de Ingeniería Agronómica, Alimentaría y de Biosistemas, UPM, Madrid, Spain

ARTICLE INFO

Keywords:
Arabidopsis thaliana
Cell wall
Disease resistance
Leucine rich repeat-malectin receptor kinases
Pattern triggered immunity
Pseudomonas syringae
Xylans
Xylotetraose

ABSTRACT

Pattern-Triggered Immunity (PTI) in plants is activated upon recognition by Pattern Recognition Receptors (PRRs) of Damage- and Microbe-Associated Molecular Patterns (DAMPs and MAMPs) from plants or microorganisms, respectively. An increasing number of identified DAMPs/MAMPs are carbohydrates from plant cell walls and microbial extracellular layers, which are perceived by plant PRRs, such as LysM and Leucine Rich Repeat-Malectin (LRR-MAL) receptor kinases (RKs). LysM-RKs (e.g. CERK1, LYK4 and LYK5) are needed for recognition of fungal MAMP chitohexaose (β-1,4-D-(GlcNAc)$_6$, CHI6), whereas IGP1/CORK1, IGP3 and IGP4 LRR-MAL RKs are required for perception of β-glucans, like cellotriose (β-1,4-D-(Glc)$_3$, CEL3) and mixed-linked glucans. We have explored the diversity of carbohydrates perceived by *Arabidopsis thaliana* seedlings by determining PTI responses upon treatment with different oligosaccharides and polysaccharides. These analyses revealed that plant oligosaccharides from xylans [β-1,4-D-(xylose)$_4$ (XYL4)], glucuronoxylans and α-1,4-glucans, and polysaccharides from plants and seaweeds activate PTI. Cross-elicitation experiments of XYL4 with other glycans showed that the mechanism of recognition of XYL4 and the DAMP 3^3-α-L-arabinofuranosyl-xylotetraose (XA$_3$XX) shares some features with that of CEL3 but differs from that of CHI6. Notably, XYL4 and XA$_3$XX perception is impaired in *igp1/cork1, igp3* and *igp4* mutants, and almost not affected in *cerk1 lyk4 lyk5* triple mutant. XYL4 perception is conserved in different plant species since XYL4 pre-treatment triggers enhanced disease resistance in tomato to *Pseudomonas syringae* pv *tomato* DC3000 and PTI responses in wheat. These results expand the number of glycans triggering plant immunity and support IGP1/CORK1, IGP3 and IGP4 relevance in *Arabidopsis thaliana* glycans perception and PTI activation.

Significance Statement: The characterization of plant immune mechanisms involved in the perception of carbohydrate-based structures recognized as DAMPs/MAMPs is needed to further understand plant disease resistance modulation. We show here that IGP1/CORK1, IGP3 and IGP4 LRR-MAL RKs are required for the perception of carbohydrate-based DAMPs β-1,4-D-(xylose)$_4$ (XYL4) and 3^3-α-L-arabinofuranosyl-xylotetraose (XA$_3$XX), further expanding the function of these LRR-MAL RKs in plant glycan perception and immune activation.

* Corresponding authors at: Centro de Biotecnología y Genómica de Plantas, Universidad Politécnica de Madrid UPM) - Instituto Nacional de Investigación y Tecnología Agraria y Alimentaria (INIA/CSIC).
E-mail addresses: pfcalvo@mbg.csic.es (P. Fernández-Calvo), antonio.molina@upm.es (A. Molina).
[1] Current address: Misión Biológica de Galicia, Consejo Superior de Investigaciones Científicas (CSIC).
[2] Current address: Umea Plant Science Center, Umea University, Sweden.
[3] Current address: Área de Fisiología Vegetal, Departamento de Ingeniería y Ciencias Agrarias, Universidad de León, León, Spain.

https://doi.org/10.1016/j.tcsw.2024.100124
Received 22 February 2024; Received in revised form 3 April 2024; Accepted 3 April 2024
Available online 4 April 2024

Introduction

Plants have a complex immune system that comprises several layers of defence that function cooperatively to confer broad-spectrum disease resistance to pathogens and pests (Ngou et al., 2022). One of these plant immunity layers is the so-called Pattern-Triggered Immunity (PTI). PTI is based on the recognition of Damage- and Microbe-Associated Molecular Patterns (DAMPs and MAMPs) derived from plants or microorganisms, respectively, by plant plasma membrane-resident Pattern Recognition Receptors (PRRs) (Nguyen et al., 2021) PRRs are modular proteins that harbour an extracellular Ectodomain (ECD) connected to a transmembrane domain (TMD), as it occurs in Receptor-Like proteins (RLPs). Some PRRs (i.e. Receptor Kinases or RKs) can also have, in addition to ECD and TMD, a cytoplasmic kinase domain (KD) (del Hierro et al., 2021). Upon DAMP/MAMP recognition by the specific ECD-PRR, the formation of an active PRR complex with additional co-receptor proteins (e.g., RKs or RLPs) occurs leading to the activation of protein kinase signalling cascades [e.g. involving Mitogen-Activated Protein Kinases (MPKs) or Calcium-Dependent Protein Kinases (CDPKs)], which in turns trigger gene reprogramming and disease resistance responses (Bigeard et al., 2015; Boutrot and Zipfel, 2017). The importance of PTI in plant defence is illustrated by the fact that disease resistance to pathogens is compromised in plants defective in PRRs and/or in their counterpart co-receptors. For example, *Arabidopsis thaliana* mutants impaired either in FLS2 RK, which is the PRR recognizing bacterial flg22 MAMP peptide through its Leucine-Rich Repeats (LRR) ECD, or in its LRR-RK co-receptor BAK1, are more susceptible to bacterial pathogens (Gómez-Gómez and Boller, 2000; Kemmerling et al., 2007). Similarly, *Arabidopsis thaliana* mutants impaired in LysM-RKs CERK1, LYK5 or LYK4, which are required for the perception of chitin oligosaccharides (e.g. β-1,4-D-$(GlcNAc)_{6\text{-}8}$, CHI6-CHI8) from fungal walls, have been described to be slightly more susceptible to fungal pathogens (Miya et al., 2007; Cao et al., 2014). PTI has been shown recently to cooperate in disease resistance with Effector Trigger Immunity (ETI) which is activated upon recognition of effector molecules from pathogens by cytoplasmic plant receptors (Yuan et al., 2021). Some of the pathogens' virulence effectors target PTI components to interfere with plant immune activation and/or to block up/hinder the crosstalk between ETI-PTI defensive responses (Yuan et al., 2021; Ngou et al., 2022).

Many PRR/peptidic DAMP/MAMP pairs triggering PTI have been characterized (Boutrot and Zipfel, 2017; Tang and Wang, 2017; Hou et al., 2019; Tanaka and Heil, 2021). In addition to peptidic ligands, plant PRRs can recognize and bind DAMPs/MAMPs of different biochemical nature like carbohydrates, lipids and other molecules (Boutrot and Zipfel, 2017; Tang and Wang, 2017). The number of carbohydrate-based DAMPs and MAMPs that have been described to be recognized by the plant immune system has increased in the last few years. However, our knowledge of the specific mechanisms of plant defence activation by carbohydrate-based ligands is behind our understanding of peptide ligands (DAMPs/MAMPs) recognition by plant PRRs (Bacete et al., 2018; Lee and Santiago, 2023). Oligosaccharide structures present in plant cell walls and microbial extracellular layers are quite diverse and can be released or modified by the activity of cell wall degrading or modifying enzymes (CWDEs) from microorganisms that target plant wall polysaccharides, or by the activity of plant enzymes that target plant and/or microbial walls/extracellular layers (aKraemer et al., 2021; Chandrasekar et al., 2022). Despite the potential diversity of glycan structures in nature that can be perceived as DAMPs/MAMPs by plants, only a few ones have been characterized so far. Among glycans perceived by plants, and in particular by *Arabidopsis thaliana*, are chitin oligosaccharides (chitohexaose, CHI6), linear β-1,3-glucans (i.e. laminarinhexaose), β-1,3-glucans with β-1,6-glucan branches, and β-1,6-glucan oligosaccharides from fungal/oomycete cell walls and peptidoglycan from bacterial walls (Klarzynski et al., 2000; Kaku et al., 2006; Aziz et al., 2007; Gust et al., 2007; Mélida et al., 2018; Wanke et al., 2020; Chaube et al., 2022). Also, plant immune system perceives oligosaccharides derived from plant cell walls polymers (DAMPs) like cellulose [β-1,4-glucan; β-1,4-D-$(Glc)_{3\text{-}5}$ or CEL3-CEL5], mixed-linked glucans [MLGs: β-1,4-D-$(Glc)_2$-β-1,3-D-Glc (MLG43), β-1,4-D-$(Glc)_3$-β-1,3-D-Glc (MLG443)], xyloglucans, xylans, mannans, arabinoxylans (e.g. 3^3-α-L-arabinofuranosyl-xylotetraose or XA_3XX) and homogalacturonans [e.g. oligogalacturonides (OGs) like $GalA_3$] (Klarzynski et al., 2000; Kaku et al., 2006; Aziz et al., 2007; Galletti et al., 2008; Claverie et al., 2018; Voxeur et al., 2019; Zang et al., 2019; Mélida et al., 2020; Malivert et al., 2021; Rebaque et al., 2021; Moussu et al., 2023; Pring et al., 2023). Moreover, some additional plant sugars that are not present in plant cell walls, like fructans, are perceived by plant cells and trigger signalling responses (Dobrange et al., 2019; Benkeblia, 2020), and some seaweed glycan structures of high molecular weight, like sulfated fucans (fucoidans) and alginates, have been also shown to active defensive responses in some plant species (Klarzynski et al., 2000; Aitouguinane et al., 2020; Aitouguinane et al., 2023; Wang et al., 2023).

In plants, PRR/carbohydrate ligand characterization at the structural level has been mainly restricted to PRRs of the LysM-RK family, which harbour ECDs with three LysM domains and have been involved in the recognition of several DAMPs/MAMPs including chitin oligomers (CHI6-CHI8), peptidoglycans, lipopolysaccharides, and lipochitooligosaccharides (MYC and Nod factors triggering symbiosis). LysM-RKs are also required for the perception of MLGs and β-1,3-glucan oligosaccharides (Miya et al., 2007; Willmann et al., 2011; Liu et al., 2012; Cao et al., 2014; Desaki et al., 2018; Mélida et al., 2018; Wanke et al., 2020). Specifically, β-1,3-glucan hexasaccharide (LAM6), MLG43 and MLG443 are immune-active structures whose recognition depends on *Arabidopsis thaliana* LysM-PRR CERK1 (Chitin Elicitor Receptor Kinase 1) (Mélida et al., 2018; Rebaque et al., 2021). However, direct binding of LAM6 and/or MLG43 to CERK1 ECD has not been either observed in Isothermal Titration Calorimetry (ITC) binding assays performed with purified ECD-CERK1 or predicted using *in silico* structural molecular dynamics simulations (del Hierro et al., 2021). Similarly, rice LysM RKs have been described to be required for the perception and binding of CHI6 and MLGs (e.g. MLG43) (Yang et al., 2021a). In addition to LysM-RKs, some Wall Associated Kinases (WAKs) and Malectin-Like RKs (e.g. FERONIA, FER) have been involved in the activation of adaptative response triggered by pectin-derived oligosaccharides, though a direct binding of the corresponding $GalA_n$ glycans to their ECDs has not been demonstrated (Malivert et al., 2021; Moussu et al., 2023). Recently, Dai and colleagues (2023) reported that the Lectin-RK OsLecRK1 is required to perceive MLGs in rice, and that OsLecRK1 produced in bacteria binds *in vitro* MLGs, but the corresponding ortholog has not been identified in *Arabidopsis thaliana* yet.

In addition to these RKs involved in oligosaccharides perception, several *Arabidopsis thaliana* RKs with Leucine-Rich-Repeat (LRR) and Malectin (MAL) domains in their ECDs have been recently characterized as components of novel recognition mechanisms for both cellulose and MLG-derived oligosaccharides (Tseng et al., 2022; Martín-Dacal et al., 2023). Several *Arabidopsis thaliana* mutants *i*mpaired in *g*lycan *p*erception (*igp; igp1-igp7*) were isolated in genetic screening to identify proteins (e.g. PRRs) required for immune activation triggered by MLG43 and CEL3, but not by CHI6 (Martín-Dacal et al., 2023). *igp1, igp3* and *igp4* were found to be altered in three LRR-MAL RKs [AT1G56145 (IGP1/CORK1 (Cello Oligosaccharide Receptor Kinase 1), AT1G56130 (IGP2/IGP3), and AT1G56140 (IGP4)] (Martín-Dacal et al., 2023). The ECD of IGP1 binds CEL3 and CEL5, but not MLG43 in ITC assays, supporting IGP1′s function as a PRR for cellulose oligosaccharides recognition and probably as a co-receptor for MLG43 perception (Martín-Dacal et al., 2023). LRR-MAL RK family comprises 13 putative members in *Arabidopsis thaliana*, with some of them involved in the regulation of pollen migration and fertility (Bordeleau et al., 2022; Lee and Santiago, 2023; Liu et al., 2024).

The potential diversity of oligosaccharide structures that are present in plant cell walls and extracellular layers of microorganisms is quite high (Wanke et al., 2020). However, only a few structures have been

demonstrated to be recognized as DAMPs/MAMPs by plants. To further characterize novel carbohydrate-based structures (MAMPs or DAMPs) perceived by plants, we tested the ability of different oligosaccharide structures to trigger early PTI responses in *Arabidopsis thaliana*. We show that oligosaccharides derived from plant polysaccharides like xylans, glucuronoxylans, arabinogalactans, and maltose-based glucans are perceived by the *Arabidopsis thaliana* immune system. Notably, we demonstrate that perception of DAMPs containing β-1,4-D-(xylose)$_n$, like XYL4 and XA$_3$XX (Mélida et al., 2020), is impaired in *igp1/cork1, igp3* and *igp4* mutants, further expanding the function of these LRR-MAL RKs beyond β-glucan perception in plants. This work expands the diversity of characterized glycans perceived as DAMPs by plants and supports the relevance of IGP1, IGP3 and IGP4 LRR-MAL RKs in plant immunity.

Material and methods

Biological material and growth conditions

Arabidopsis thaliana lines used in this study were in the Columbia-0 (Col-0) background. The following *Arabidopsis thaliana* plants carrying the calcium reporter aequorin were used for cytoplasmic calcium (cyt Ca^{2+}) measurements: Col-0^{AEQ} (Knight et al., 1991), *cerk1-2*^{AEQ} (Ranf et al., 2012), and *igp1*^{AEQ}, *igp3*^{AEQ} and *igp4*^{AEQ} (Martín-Dacal et al., 2023). The *cerk1-2 lyk4-1 lyk5-1* triple mutant used was previously obtained in the lab (Martín-Dacal et al., 2023). For MAPKs phosphorylation and gene expression analyses Col-0 wild-type (WT) and mutant seedlings were grown in 24-well plates (~10 seedlings per well) under long-day conditions (16 h of light: 8 h of darkness) at 19–21 °C in liquid ½ MS medium with 1 % saccharose. Tomato plants (*Solanum lycopersicum,* Moneymaker) were grown in the greenhouse in a mixture of soil and vermiculite (3:1) at under 14 h of light/10 h of dark at 24–22 °C. Wheat plants (*Triticum aestivum* cultivar Titlis) were grown in greenhouse in soil-vermiculite (3:1) at under 14 h of light/10 h of dark at 24–19 °C.

Carbohydrates and peptides used in the experiments

Hexaacetyl-chitohexaose (CHI6; β-1,4-D-(GlcNAc)$_6$; #O-CHI6), CEL3 (β-1,4-D-(Glc)$_3$; O-CTR), xylobiose (XYL2), xylotriose (XYL3), 2^3–(4-O-Methyl-α-D-Glucuronyl)-xylotetraose (XUXX), α-D-Maltotetraose (MAL4), XA$_3$XX, and 6^3-α-D-Maltotriosyl-maltotriose (MAL3$_2$) were purchased from Megazyme (Wicklow, Ireland). β-1,4-D-Xylotetraose (XYL4) was purchased both from Megazyme (0-XTE) (Wicklow, Ireland) and Cymit Química (Barcelona, Spain). The peptide flg22 was synthesized by Abyntek (Zamudio, Spain). Oligosaccharides/polysaccharides used in the experiments are summarized in Table S1.

β-1,6-D-glucan oligosaccharides were purified from commercial pustulan polysaccharide (InvivoGen #tlrl-pst) as detailed below. Fifty mg of pustulan was added to 25 mL of 0.2 N HCl and incubated at 100 °C for 8 h. Afterwards, hydrolysates were cooled down and neutralized by adding an equal volume of 0.2 N NaOH. Digestion products were desalted and pre-purified using a Sephadex G-10 column (90 cm^3 bed-volume in a 1.5 cm diameter column; Merck) and size-fractionated using a Biogel P2 Extrafine column (140 cm^3 bed-volume in a 1.6 cm diameter column; BioRad). Columns were connected to a Biologic-LP instrument, distilled water was used as the mobile phase and the flow rates were 0.24 mL/min. Purified oligosaccharides were monitored by high-performance liquid chromatography (HPLC). The oligosaccharides were injected into an Agilent 1200 Series HPLC equipped with an Agilent 6130 quadrupole mass spectrometer (MS) and an Agilent 1200 Evaporative Light Scattering Detector (ELSD). The purified oligosaccharides were separated on a graphitized carbon Hypercarb column (150 x 4.6 mm, Thermo Scientific) using a water (including 0.1 % formic acid)-acetonitrile (ACN) gradient. The peaks in the ELSD traces were assigned based on their retention time and the corresponding masses in the MS. For additional MS analyses, a fraction of each oligosaccharide sample was injected directly into an Agilent 1260 Infinity II Series, LC/MSD XT (Single Quadrupol mit ESI-Jetstream-source).

Polysaccharides from different sources were also examined, including alginate from brown algae (Thermo Fisher Scientific; CAS: 9005-38-3; (C6H7O7)a(C6H7O7)bNa; Geel, Belgium), fucoidan from *Undaria pinnatifida* (Sigma-Aldrich; CAS:9072-19-9; Saint Louis, USA) and arabinogalactan from Larch Wood (TCI; CAS: 9036-66-2; [(C5H8O4)(C6H10O5)6]x; Tokyo, Japan). Alginate was applied at 0.5 g/L, fucoidan at 3 g/L, and arabinogalactan at 0.33 g/L.

Aequorin luminescence measurements and cross-elicitation experiments

Arabidopsis thaliana Col-0^{AEQ} 8-day-old seedlings grown in liquid medium were used for cytoplasmic calcium (cyt Ca^{2+}) measurements using the method previously described (Bacete et al., 2017). Negative controls (water = mock) were included in all the experiments. The elevation of cytoplasmic calcium concentration was measured as relative luminescence units (RLU) of aequorin luminescence with a Varioskan Lux Reader (Thermo Scientific) as described previously (Mélida et al., 2018). Cross-elicitation during the refractory period of calcium signaling upon the sequential application of two different compounds (e.g. XYL4-CEL3, XYL4-XA3XX, XYL4-CHI6, and vice versa), as well as XYL4-XYL4 (positive control), and XYL4-water (negative control) were performed as previously described (Rebaque et al., 2021).

Immunoblot analysis of MPKs activation

Twelve-day-old *Arabidopsis thaliana* seedlings from different genotypes grown on liquid MS medium in 24-well plates were treated with water (mock) and different oligosaccharides for 0, 10 and 20 min, and then harvested in liquid nitrogen. Seedlings were homogenized using FastPrep Bead Beating Systems (MP Biomedicals) in extraction buffer (50 mM Tris-HCl pH 7.5, 200 mM NaCl, 1 mM EDTA, 10 mM NaF, 2 mM sodium orthovanadate, 1 mM sodium molybdate, 10 % (v/v) glycerol, 0.1 % (v/v) Tween-20, 1 mM 1,4-dithiothreitol, 1 mM phenylmethylsulfonyl fluoride, and phosphatase inhibitor cocktail P9599 (Sigma)). Total protein extracts were quantified by Bradford assay (Bio-Rad). Equal amounts of proteins were separated on Mini-PROTEAN TGX, 10 %, 10-well, 30 μL (Bio-Rad) gel and transferred to PVDF membranes using Invitrogen™ iBlot™ 2 Gel Transfer Device. Membranes were blocked with Protein-Free (TBS) Blocking Buffer (Thermo Scientific; Pierce) for 2 h at room temperature. Membranes were incubated overnight at 4 °C in TBS containing Phospho-p44/42 MAPK (Erk1/2) (Thr202/Tyr204) antibody (Cell Signaling Technology) (1:1000) or Anti-AtMPK3 (1:2500) (Sigma-Aldrich). The latest was used as an internal control for protein loading. Membranes were cleaned fourth with TBS containing 0.1 % Tween-20 and incubated with horseradish peroxidase-conjugated anti-rabbit antibody (GE-Healthcare) (1:5000) in TBS. Membranes were cleaned again and revealed by ECL Western Blotting Substrate (Thermo Scientific; Pierce) and detected using iBright FL1000 Image System (ThermoFisher Scientific). Finally, the membranes were stained with Ponceau-S Red (Sigma Aldrich) to ensure the presence of proteins in all the lanes. Western experiments were repeated at least twice.

Gene expression analyses

For gene expression analysis (qRT-PCR and RNA sequencing), 12-day-old *Arabidopsis thaliana* seedlings grown on liquid MS medium were treated with oligosaccharides or water (mock) for 30 min. Total RNA was purified with the RNeasy Plant Mini Kit (Qiagen) according to the manufacturer's protocol. qRT-PCR analyses were performed as previously reported (Bacete et al., 2017). *UBC21* (*At5g25760*) expression was used to normalize the transcript level in each reaction. The forward and reverse sequences of the oligonucleotides used to monitor gene expression levels of *WRKY53* (*At4g23810*), *CYP81F2* (*At5g57220*) and *UBC21* (*At5g25760*) are:

WRKY53: 5́-CACCAGAGTCAAACCAGCCATTA-3́/5́-CTTTACCATCATCAAGCCCATCGG-3́;

CYP81F2: 5́-TATTGTCCGCATGGTCACAGG-3́/5́-CCACTGTTGTCATTGATGTCCG-3́;

UBC21: 5́-GCTCTTATCAAAGGACCTTCGG-3́/5́-CGAACTTGAGGAGGTTGCAAAG-3́.

For RNA-seq analyses, samples from three biological replicates for each treatment were sequenced using 50 bp Illumina Hiseq 2500. RNA-seq read data can be retrieved from the NCBI Sequence Read Archive (SRA) under BioProject accession ID PRJNA625401 (BioSample accession SAMN15682114). The initial quality control of sequencing data was evaluated using FastQC (v0.11.9) (Andrews, 2010) and multiqc (v1.7) (Ewels et al., 2016). This data was then used to filter sequences with the Trimmomatic tool (v0.36) (Bolger et al., 2014). For each sample, RNA-seq raw reads (paired-end, 150 bp) were trimmed to remove potential Illumina adaptor contamination, followed by read trimming and clipping of low-quality bases. The remaining reads were aligned to the *Arabidopsis thaliana* TAIR10 reference genome, using the Araport11 annotation (Cheng et al., 2017) with the STAR aligner (v2.5.3a) (Dobin et al., 2013) and specific command-line parameters: –outFilterMultimapNmax 20 –alignSJoverhangMin 8 –alignSJDBoverhangMin 8 –outFilterMismatchNmax 8 –alignIntronMin 35 –alignMatesGapMax 100,000 –alignIntronMax 20,000. HTSeq (v1.99.2) (Anders et al., 2010) was used with the intersection 'union' option to generate the read counts per gene, based on the RNA-seq mapped reads and the Araport11 annotation. Normalization and statistical analyses of differential gene expression were performed with the DESeq2 Bioconductor package in R (Love et al., 2014). Genes were considered differentially expressed (DEGs), as either up or down regulated, if they had a log2-fold change [log2-FC] > 0.58 with an adjusted P value ≤ 0.05. The lists of DEGs generated from DESeq2 were used to perform functional enrichment analysis against the biological process subset of the gene ontology (GO) using the 'enrichGO' function of the R package clusterProfiler (v4.2.2) (Wu et al., 2021). GO terms were considered overrepresented if their False Discovery Rate (FDR) were $\leq$ 0.05. Redundant GO terms were removed using 'simplify' function from clusterProfiler with z score cutoff of 0.5. Figures of enrichment analysis were generated by ggplot2 package (v3.4.4) (Wickham, 2016).

Tomato disease resistance assays

Tomato plants (*S. lycopersicum* Moneymaker) were grown in a greenhouse in soil-vermiculite (3:1) under 14 h of light/10 h of dark at 24–22 °C. The third and fourth leaves of three-week-old plants were sprayed with 2 mL of an XYL4 solution (450 μM) in water containing 0,1% Tween 20 (Sigma) as an adjuvant. The adjuvant solution in water was used as a mock. *Pseudomonas syringae* pv. *tomato* DC3000 infections were performed 48 h after pre-treatments according to (Santamaría-Hernando et al., 2019) Briefly, plants were sprayed with a suspension of the bacterium (10^8 cfu/ml), and two tomato leaf discs were collected from 4 different plants at 0- and 7 days post-infection (dpi). Colony forming units (cfu) per foliar area were determined after plating serial dilutions onto KB plates with rifampicin (25 μg/ml).

Determination of reactive oxygen species (ROS) production in wheat

Disks (12.6 mm2) from second leaves of 14-day-old wheat plants were pre-treated with 100 μL of 150 nM Luminol L-012 (FUJIFILM Wako Pure Chemical Corporation, 120–04891) and 15 μg/mL Peroxidase from horseradish (Sigma-Aldrich, P6782). After 16 h incubation in the dark at 15 °C, 50 μL of 750 μM XYL4, 3 μM flg22 or H_2O (control/mock) were added, and luminescence was measured using Varioskan Lux (Thermo Scientific). Eight leaf discs per treatment were used in each experiment. The experiment was performed three times independently.

Results

A diverse set of oligosaccharides trigger calcium influxes in Arabidopsis thaliana

We used the Aequorin-based cytoplasmic Ca^{2+} (Col-0^{AEQ}) sensor *Arabidopsis thaliana* system (Knight et al., 1991; Martín-Dacal et al., 2023) to expand our knowledge on plant/microbial/seaweed oligosaccharides that are perceived by the plant immune system. We measured early cytoplasmic Ca^{2+} influxes (burst) in Col-0^{AEQ} seedlings upon treatment with different oligo- and polysaccharides. Oligosaccharides tested were molecules derived from plant polysaccharides such as xylans (e.g. β-1,4-D-Xylotetraose or XYL4), glucuronoxylans (2^3–(4-O-Methyl-α-D-Glucuronyl)-xylotetraose or XUXX), and α-1,4-glucans (α-1,4-D-Glc based maltodextrins: α-D-Maltotetraose (MAL4) and 6^3-α-D-Maltotriosyl-maltotriose ($MAL3_2$)). We found that XYL4 and XUXX triggered Ca^{2+} bursts with different kinetics (Fig. 1A). XYL4 promotes a very fast Ca^{2+} burst in Col-0^{AEQ}, whereas the pentasaccharide XUXX triggered a Ca^{2+} burst similar to that of CHI6 (Fig. 1A). MAL4 and $MAL3_2$ also elicited a weak, but reproducible Ca^{2+} burst in Col-0^{AEQ} seedlings (Fig. 1A), indicating that *Arabidopsis thaliana* can perceive α-1,4-glucan-derived oligosaccharides in addition to the previously described β-glucan-derived ones (Mélida et al., 2018; Rebaque et al., 2021; Martín-Dacal et al., 2023).

To validate PTI activity of XYL4, XUXX, MAL4 and $MAL3_2$, we next monitored the phosphorylation levels of the protein kinases MPK3, MPK6, MPK4 and MPK11 and the up-regulation of PTI-associated genes (*CYP81F2* and *WRKY53*) upon treatment of *Arabidopsis thaliana* Col-0 wild-type seedlings with these active glycans. Western-blot assays confirmed MPK3- and MPK6-phosphorylation upon application of XYL4 (250 μM) to Col-0 seedlings, with the maximum phosphorylation levels reached at 20 min post-treatment (Fig. 1B). MPKs phosphorylation triggered by XYL4 was weaker than those observed after treatment with CHI6 included for comparison (Fig. 1B). MPK4/11-phosphorylation was almost not-detectable in XYL4-treated plants, which contrasted with the observed phosphorylation of these MPKs in Col-0 plants upon CHI6 treatment (Fig. 1B). MAL4 triggered MPKs phosphorylation to a similar level than XYL4 (Fig. 1B), whereas XUXX and $MAL3_2$ triggered weaker MPKs phosphorylation than XYL4 (Fig. 1B). Expression of two PTI-marker genes (*WRKY53* and *CYP81F2*), that are up-regulated by several glycans (Mélida et al., 2018), was assessed by qRT-PCR in *Arabidopsis thaliana* Col-0 seedlings 30 min after treatment with these oligosaccharides or with water (mock). Of note, we found that these two genes were up regulated after treatment with the four analysed glycans (Fig. 1C). The level of up-regulation of *WRKY53* and *CYP81F2* upon XYL4 or MAL4 treatment was very similar to those observed after CHI6 treatment (Fig. 1C), whereas XUXX and $MAL3_2$ triggered weaker up-regulation of these marker genes (Fig. 1C), which is in line with the faint phosphorylation of MPK bands observed in Western blot analyses (Fig. 1B). These results further indicated that XUXX and $MAL3_2$ are not very active DAMPs in *Arabidopsis thaliana*.

To expand the list of active oligosaccharides triggering PTI in *Arabidopsis thaliana*, we also measured early cytoplasmic Ca^{2+} influxes (burst) in Col-0^{AEQ} seedlings upon treatment with additional glycans/polysaccharides with distinct composition/structure. We tested the effect on Ca^{2+} influxes of purified β-1,6-D-$(Glc)_{3-4}$ oligosaccharides from bacterial pustulan (Fig. S1A, and different polysaccharides from plants (arabinogalactans) and seaweed (fucoidan and low molecular weight alginates). We purified β-1,6-D-(Glc) oligosaccharides with different Degree of Polymerization [DP: β-1,6-D-$(Glc)_{3-4}$; Fig. S1A] and demonstrated that they triggered weak Ca^{2+} burst and MPK phosphorylation (Fig. S1B, C), further confirming that plants perceive β-1,6 glucan structures (Chaube et al., 2022) in addition to lineal β-1,3 and branched β-1,3/β-1,6 glucans, which are present in laminarin and some fungal cell wall glycans (Mélida et al., 2018; Wanke et al., 2020; Wanke et al., 2023). Moreover, we found that arabinogalactans, fucoidans, and

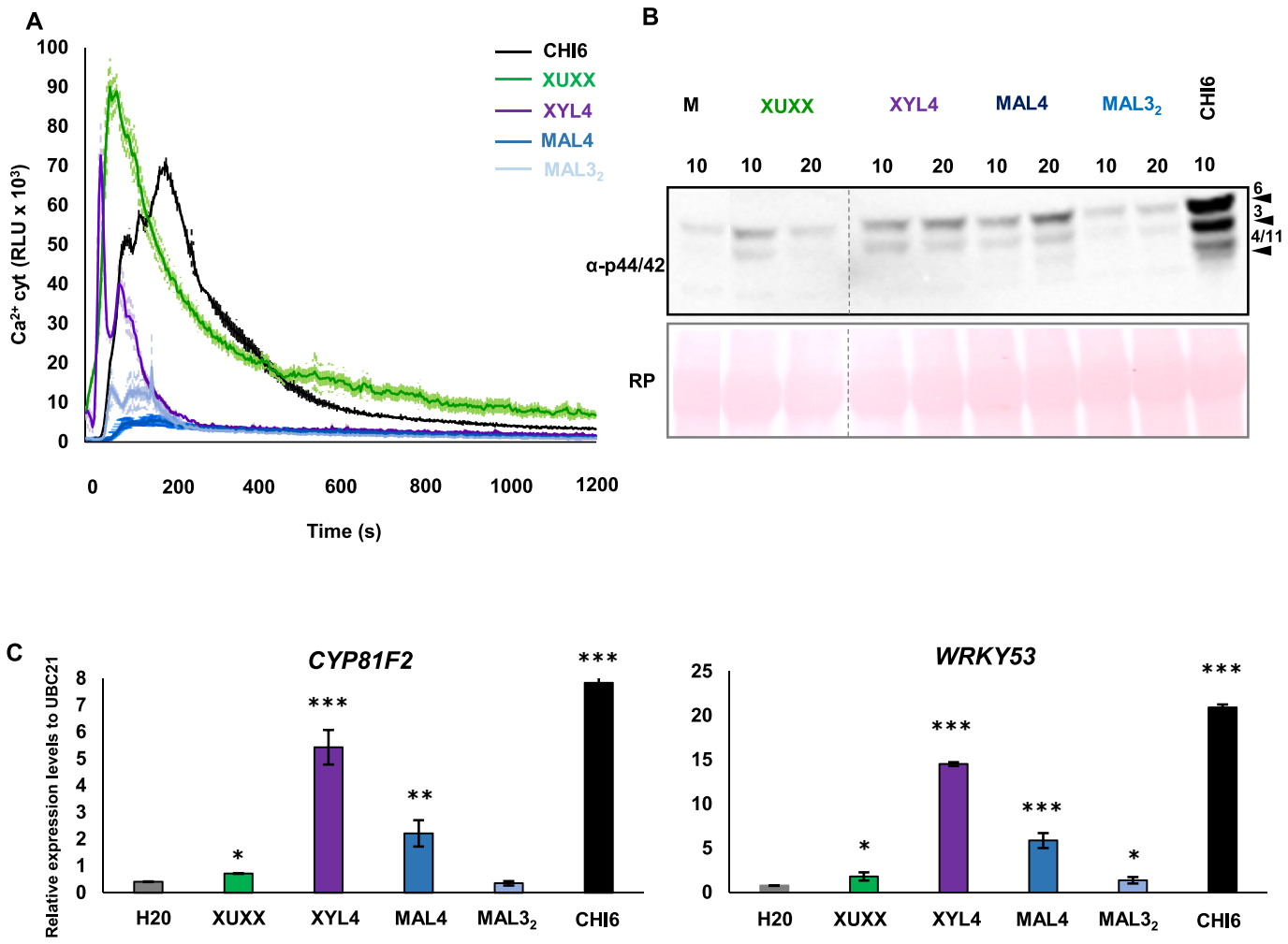

Fig. 1.

Fig. 1. Xylotetraose (XYL4) activates immune hallmarks in *Arabidopsis thaliana*. (A) Cytoplasmic calcium (cyt Ca^{2+}) influx was measured as relative luminescence units (RLU) over time in 8-days-old *Arabidopsis* Col-0 ^{AEQ} (WT) treated with 250 μM of candidate oligosaccharides: 2^3-(4-O-Methyl-α-D-Glucuronyl)-xylotetraose (XUXX), β-1,4-D-Xylotetraose (XYL4), α-D-Maltotetraose (MAL4), 6^3-α-D-Maltotriosyl-maltotriose ($MAL3_2$) and chitin (CHI6, 50 μM). (B) Phosphorylation of mitogen-activated protein kinases (MPKs) analysed by Western-blot (WB) in seedlings treated with the indicated compounds or water (mock) and harvested at 10 and 20 min after treatment application. Dotted lines indicate that bands were cut from the membrane to relocate them in proper order. (C) PTI-related gene expression (*CYP81F2* and *WRKY53*) measured by RT-quantitative PCR at 30 min after compound application. Similarly, water-treated seedlings were analysed as negative controls. Data represent (A) the mean ± error standard (n = 8) of a representative experiment, (B) representative WB out of two independent experiments performed, and (C) the mean ± error standard (n = 3) of three independent experiments. Statistically significant differences between compound-treated plants versus mock-treated (M, H_2O) were calculated according to Student's *t*-test (*P < 0.05, **0.01 < P > 0.001, ***P < 0.001).

alginates induced Ca^{2+} bursts, though these responses were observed only at very high concentrations (mM level) of these compounds (Fig. S2A). Hence our data confirmed the previously described elicitor activity of fucoidans and alginates in different plant species (Klarzynski et al., 2000; Aitouguinane et al., 2020; Aitouguinane et al., 2023; Wang et al., 2023) and highlighted the appropriateness of *Arabidopsis thaliana* as a suitable system to study the mechanisms of perception of these glycans and the PRRs involved in their recognition.

Mechanism of perception of XYL4 share some components with those of CHI6, CEL3 and XA_3XX

Provided that XYL4 triggered a strong and consistent response in Ca^{2+} input, gene expression levels and MAPK phosphorylation, we further determine the specificity of PTI responses triggered by XYL4 and decipher its mechanism of perception by *Arabidopsis thaliana*. We performed cross-elicitation experiments, using Col-0^{AEQ} seedlings, treated with XYL4, CEL3 CHI6, and the DAMP arabinoxylan-derived pentasaccharide XA_3XX previously described (Mélida et al., 2020). In these experiments, we measured Ca^{2+} burst in Col-0^{AEQ} seedlings after the sequential application of different glycans (Mélida et al., 2020; Rebaque

et al., 2021). As shown in control treatment XYL4-XYL4, a total reduction of second Ca^{2+} burst (refractory response) was observed upon the second treatment of plants with XYL4, showing an RLU kinetic that was similar to that of XYL4-H_2O control treatment (Fig. 2A, B). Remarkably, a strong refractory response was observed in the XYL4-CEL3 combination (Fig. 2C), which was similar to that of XYL4-XYL4 treatment (Fig. 2 A). Still, the intensity of CEL3 Ca^{2+} burst is stronger than that of XYL4 and accordingly sequential application of XYL4-CEL3 did not completely abolish CEL3 triggered Ca^{2+} burst in contrast to CEL3-XYL4 sequential application (Fig. 2C). Of note, these results suggest that the mechanisms of recognition of XYL4 overlap with those of CEL3, which involve the recently characterized IGP1/IGP3/IGP4 LRR-MAL RKs (Martín-Dacal et al., 2023). In contrast, a weak refractory response (reduction of Ca^{2+} burst) was observed when XYL4 and CHI6 were sequentially applied to Col-0^{AEQ} seedlings (Fig. 2D), suggesting that the mechanisms of perception of XYL4 and CHI6 are not identical, but might share some LysM-RK components (Fig. 2B). Notably, Col-0^{AEQ} seedlings showed strong refractory responses when XYL4-XA_3XX were combined (Fig. 2E), but the observed reduction of Ca^{2+} burst was not total in comparison to that observed in the control experiments (XYL4-XYL4: Fig. 2A). Additionally, these data indicated that XYL4 shares some receptor components required for XA_3XX perception, that have not been yet identified. Together these data suggest that β-1,4-D-Xyl-based oligosaccharides (i.e. XYL4 and XA_3XX) and oligosaccharides with β-1,4-D-Glc bonds (i.e. CEL3 and MLG43) might share some perception mechanisms.

The mechanism of XYL4 perception in Arabidopsis thaliana depends on IGP1/IGP3/IGP4 LRR-MAL RKs

To further unravel the perception mechanism of XYL4 in *Arabidopsis thaliana* we tested XYL4-mediated cytoplasmic Ca^{2+} burst in *igp1*^{AEQ}, *igp3*^{AEQ} and *igp4*^{AEQ} mutant lines. *igp1*^{AEQ} is impaired in IGP1/CORK1, the probed PRR pair for CEL3/CEL5 DAMPs ((Martín-Dacal et al., 2023). Likewise, *igp3*^{AEQ} and *igp4*^{AEQ} are defective in IGP3 and IGP4 RKs that might function as co-PRRs in CEL3/CEL5 perception. These three LRR-MAL RKs are also required for MLG43 perception (Martín-Dacal et al., 2023). We monitored early cytoplasmic Ca^{2+} influx (burst) in these mutants upon XYL4 treatment and found that Ca^{2+} influx in *igp3*^{AEQ} and *igp4*^{AEQ} lines was fully impaired upon XYL4 treatment, whereas in *igp1*^{AEQ} plants a significant reduction of the burst was observed in comparison to Col-0^{AEQ} plants (Fig. 3A), as observed previously for CEL3 and MLG43 perception (Martín-Dacal et al., 2023). Next, we tested MPKs phosphorylation by western blot in *igp1*^{AEQ}, *igp3*^{AEQ,} and *igp4*^{AEQ} lines and Col-0^{AEQ} plants upon XYL4 treatment in comparison with CHI6- and mock-treated plants. We found that MPKs phosphorylation levels were weaker in the *igp1*^{AEQ}, *igp3*^{AEQ,} and *igp4*^{AEQ} mutants than in Col-0^{AEQ} plants upon XYL4 treatment, whereas phosphorylation triggered by CHI6 was not significantly affected in these *igp* mutants, as reported [Fig. 3B; (Martín-Dacal et al., 2023)]. This prompted us to also test the up-regulation of two PTI marker genes (i.e. *CYP81F2* and *WRKY53*) upon XYL4 treatment in *igp* mutants and Col-0 wild-type plants. We found that up-regulation of such genes was also impaired in *igp* mutants in comparison to Col-0 plants (Fig. 3C). These data confirm that the LRR-MAL RKs (IGP1/CORK1, IGP3, and IGP4), that are required for CEL/MLG43-dependent PTI activation, also play a role in XYL4 perception, further expanding the function of this novel group of LRR-MAL RK in the perception of additional glycans.

XA_3XX perception in Arabidopsis thaliana also depends on IGP1/IGP3/IGP4 LRR-MAL RKs

Refractory experiments suggested similarities between XYL4 and XA_3XX perception mechanisms (Fig. 2C). Additionally, the involvement of IGP1/IGP3/IGP4 RKs in XYL4 recognition by *Arabidopsis thaliana* points to a broader role of such RKs in oligosaccharide perception. Therefore, we questioned whether these RKs might be also involved in XA_3XX recognition by plants. We used Col-0^{AEQ}, *igp1*^{AEQ}, *igp3*^{AEQ,} and *igp4*^{AEQ} lines to monitor early cytoplasmic Ca^{2+} influx in these mutants upon XA_3XX treatment. Notably, Ca^{2+} influxes in XA_3XX-treated *igp1*^{AEQ}, *igp3*^{AEQ}, and *igp4*^{AEQ} seedlings were reduced in comparison to those in Col-0^{AEQ} (Fig. 4A). The reductions observed upon XA_3XX treatment were similar to those observed after treatment of these plants with XYL4, with stronger impairment in *igp3*^{AEQ} and *igp4*^{AEQ} than in *igp1*^{AEQ} (Fig. 3A), as previously described for CEL3 and MLG43 (Martín-Dacal et al., 2023). Next, we tested the phosphorylation of MPKs by western blot in *igp1*^{AEQ}, *igp3*^{AEQ}, *igp4* and Col-0 plants upon XA_3XX treatment. We found that MPKs phosphorylation levels were reduced in the *igp1*^{AEQ}, *igp3*^{AEQ} and *igp4* mutants in comparison to wild-type (Col-0) plants, and that this reduction was weaker in *igp1* ^{AEQ} than in *igp3* ^{AEQ} and *igp4* plants (Fig. 4B). As described previously, MPKs phosphorylation triggered by CHI6 treatment, included as a control, was not impaired in the *igp* mutants (Fig. 4B). In agreement with MPKs phosphorylation levels, we found that the observed up-regulation of PTI marker genes *CYP81F2* and *WRKY53* upon treatment of Col-0 plants with XA_3XX was significantly impaired in *igp3* ^{AEQ} and *igp4* mutants, whereas such reduction was milder in *igp1*^{AEQ} plants (Fig. 4C). These data indicate that IGP1, IGP3 and IGP4 RKs, which are required for PTI activation mediated by CEL/MLG43 (Martín-Dacal et al., 2023)and XYL4 (Figs. 1 and 3), also play a function in XA_3XX perception in *Arabidopsis thaliana*.

Since LRR-MAL RKs are required for the perception of different oligosaccharides, we tested whether the perception of arabinogalactan, fucoidans, and alginates, that trigger PTI responses in *Arabidopsis thaliana* [Fig. S2; (Wang et al., 2023)] was dependent on these LRR-MAL RKs. We used Col-0^{AEQ}, *igp1*^{AEQ} and *igp4*^{AEQ} lines (Martín-Dacal et al., 2023) to monitor early cytoplasmic Ca^{2+} influx and upon treatment with these polysaccharides. We found that Ca^{2+} influxes were not impaired in *igp1*^{AEQ} and *igp4*^{AEQ} lines, further indicating that at least IGP1/CORK1and IGP4 are not required for the perception of these plant/seaweed-derived DAMPs (Fig. S2B). To further corroborate these data, we determined phosphorylation of MPKs by western blot in *igp1*^{AEQ}, *igp4* and Col-0 plants upon treatment with these polysaccharides. We found that MPKs phosphorylation levels were not impaired in the *igp1*^{AEQ} and *igp4* mutants in comparison to wild-type (Col-0) plants, which contrasted with the observed reduction of MPKs phosphorylation observed in mutants treated with CEL3 (Fig. S2C). These data further confirmed that IGP1/CORK1 and IGP4 are not required for the perception of these plant-derived (arabinogalactan) and seaweed-derived (fucoidans and alginates) glycans. Hence additional mechanisms, yet unknown, might be involved in the perception of these polysaccharides by plants.

XYL4 and XA_3XX perception in Arabidopsis thaliana depends partially on CERK1, LYK4 and LYK5 LysM receptors

The refractory experiments between XYL4 and CHI6 suggested that the mechanism of perception of these two glycans might share some components (Fig. 2C). Accordingly, we used Col-0^{AEQ} and *cerk1-2*^{AEQ} lines to monitor whether early cytoplasmic Ca^{2+} influxes were impaired in *cerk1-2*^{AEQ} upon XYL4 and XA_3XX treatments. Notably, XYL4 and XA_3XX triggered Ca^{2+} influxes in *cerk1-2*^{AEQ} seedlings whereas CHI6 did not (Fig. 5A), as described previously (Mélida et al., 2020). Since LysM proteins CERK1, LYK5 and LYK4 play redundant functions in CHI6 perception (Miya et al., 2007; Cao et al., 2014; Mélida et al., 2018), we used *cerk1-2 lyk4-1 lyk5-1* triple mutant to test MPKs phosphorylation upon XYL4 and XA_3XX treatments. As shown in Fig. 5B, phosphorylation of MPKs in *cerk1-2 lyk4-1 lyk5-1* mutant upon CHI6 treatment was fully impaired, as predicted from the requirement of CERK1, LYK4 and LYK5 for its perception (Martín-Dacal et al., 2023). In contrast, phosphorylation of MPKs in the LysM triple mutant upon XYL4 or XA_3XX treatment was only slightly reduced (Fig. 5B) indicating that these receptors play some minor function in the perception of xylose-containing glycans in *Arabidopsis thaliana*. In line with this minor function of LysM-RKs, the up-regulation of the PTI marker genes *CYP81F2* and *WRKY53* in *cerk1-2 lyk4-1 lyk5-1* lines upon XYL4 or XA_3XX treatment was not significantly different from that observed in Col-0 plants (Fig. 5C). These results also

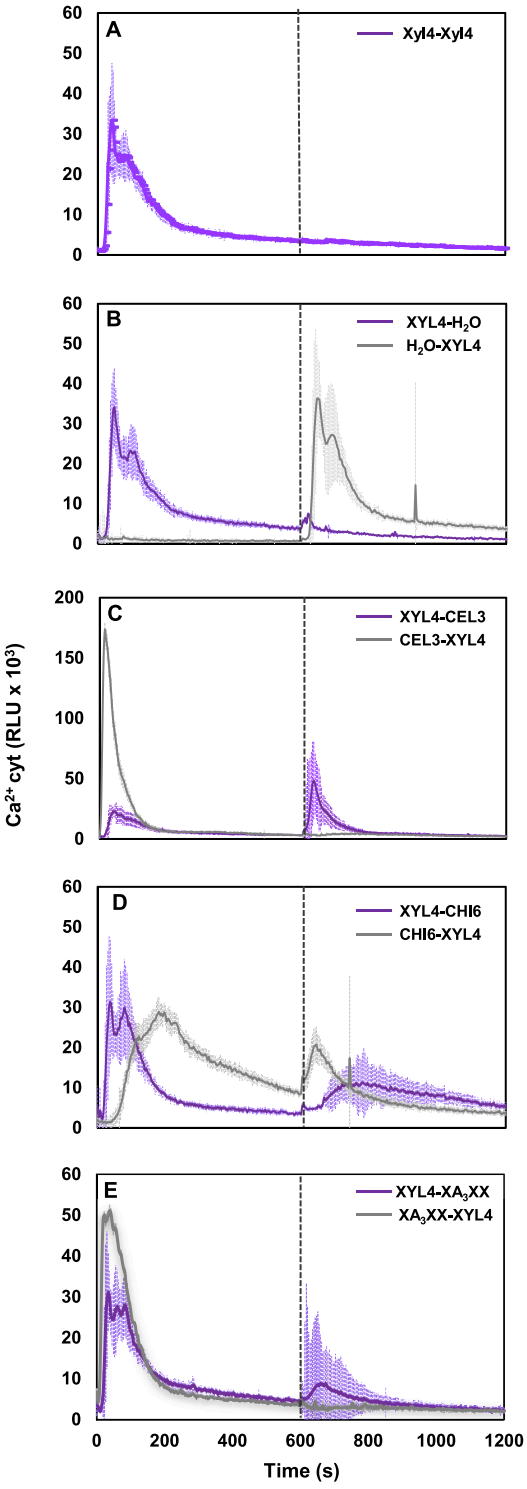

Fig. 2.

(caption on next column)

Fig. 2. Cross-elicitation during the refractory period of calcium burst triggered by XYL4 in combination with CEL3, CHI6, and/or XA_3XX. Cyt Ca^{2+} burst (RLU) over time in 8-day-old Col-0^{AEQ} seedlings after sequential treatments with 250 μM XYL4 followed by 250 μM XYL4 (A), WATER (B), 10 μM CEL3 (C), 50 μM CHI6 (D), or 250 μM XA_3XX (E) and vice versa. A and B panels represent the negative and positive controls of the experiment, respectively. XYL4 as the first treatment applied is indicated in purple and any other compound and/or water added is indicated in grey. Pointed lines indicate the application time of the second glycan/water. Data represent the average RLU values of 4 seedlings (n = 4) ± standard deviation. This is a representative experiment of the two performed that gave similar results. (For interpretation of the references to colour in this figure legend, the reader is referred to the web version of this article.)

demonstrated that the mechanisms of perception of XYL4/XA_3XX and CHI6 are different.

XYL4 triggered defensive responses in different plant species

To further characterize the basis of XYL4-mediated PTI activation, we performed RNA-seq analyses of Col-0 seedlings treated for 30 min with XYL4, CEL3, CHI6 or water (Mock: Fig. 6, Table S2-S3-S4). XYL4 triggered the differential expression of 185 genes (DEGs), most of which (154) were up-regulated (Fig. S6A and Table S2). On the other hand, treatments either with CEL3 or CHI6 resulted in 679 and 581 DEGs, respectively (Table S3 and S4, Fig. 6), most of them up-regulated (562 by CEL3- and 532 by CHI6-treatment). The overlapping of DEGs among the three compounds, as shown in the Venn Diagram (Fig. 6A, B), strongly points to shared molecular components in the signalling mechanisms activated by XYL4 and CEL3/CHI6, as shown above in cross-elicitation experiments (Fig. 2). XYL4 up-regulated genes mainly grouped into gene ontology (GO) terms related to immune system processes, and response to different stimuli, including biotic and abiotic stresses, among other GOs (Fig. 6B). Likewise, similar enriched GOs were found in response to CEL3 and CHI6, which shared DEGs between them and with XYL4 (Fig. S3 and Table S5). Overall, these analyses indicate that the transcriptional reprogramming triggered by XYL4 overlaps partially with that induced by other well-known DAMPs and MAMPs, such as CEL3 and/or CHI6, though with specific DEGs and GOs. The majority of shared DEGs upon XYL4, CEL3 and CHI6 treatment are immune and stress related genes (Table S5) further confirming the function of these glycans in the regulation of plant disease resistance. Among XYL4 specific DEGs some encoded RLPs/RKs and other stress-associated proteins (Table S6). Together these data indicate that the mechanism of XYL4 perception shares some similar components (e.g. RKs) but is not identical to that of CEL3 and/or CHI6, as indicated by the cross-elicitation and genetics experiments (Figs. 2, 3, and 5).

XA_3XX has been shown previously to trigger disease resistance in tomatoes and peppers against bacterial and fungal pathogens, respectively (Mélida et al., 2020). XYL4, like XA_3XX oligosaccharide, can be released from plants cell walls upon pathogen infection by the activity of *endo*-xylanases or arabinoxylanases (e.g., GH11) secreted by these pathogens during colonization, as suggested recently (Mélida et al., 2020; Pring et al., 2023). Therefore, we tested the elicitor activity of XYL4 in three-week-old tomato plants (var. Moneymaker), which were treated by foliar spray with XYL4 two days prior spray-inoculation with the virulent bacterium *Pseudomonas syringae* pv. *tomato* DC3000. Notably, bacterial population, determined as colony forming units (cfu) per leaf area (cm^2), was significantly reduced in the XYL4-pretreated tomato plants at 7 days post inoculation compared to mock-treated plants (Fig. S4). We also tested if xylooligosaccharides (XYL4, XYL3 and XYL2) were perceived by monocot crops (i.e. wheat) by determining the production of reactive oxygen species (ROS), one of the PTI hallmarks in plants, upon treatment of wheat leaf discs with these glycans. As shown in Fig. 7, XYL4 triggered ROS production in wheat leaf discs that was weaker than that induced by MAMP flg22 used as a control MAMP in the experiment. In contrast, XYL2 and XYL3 were not active in

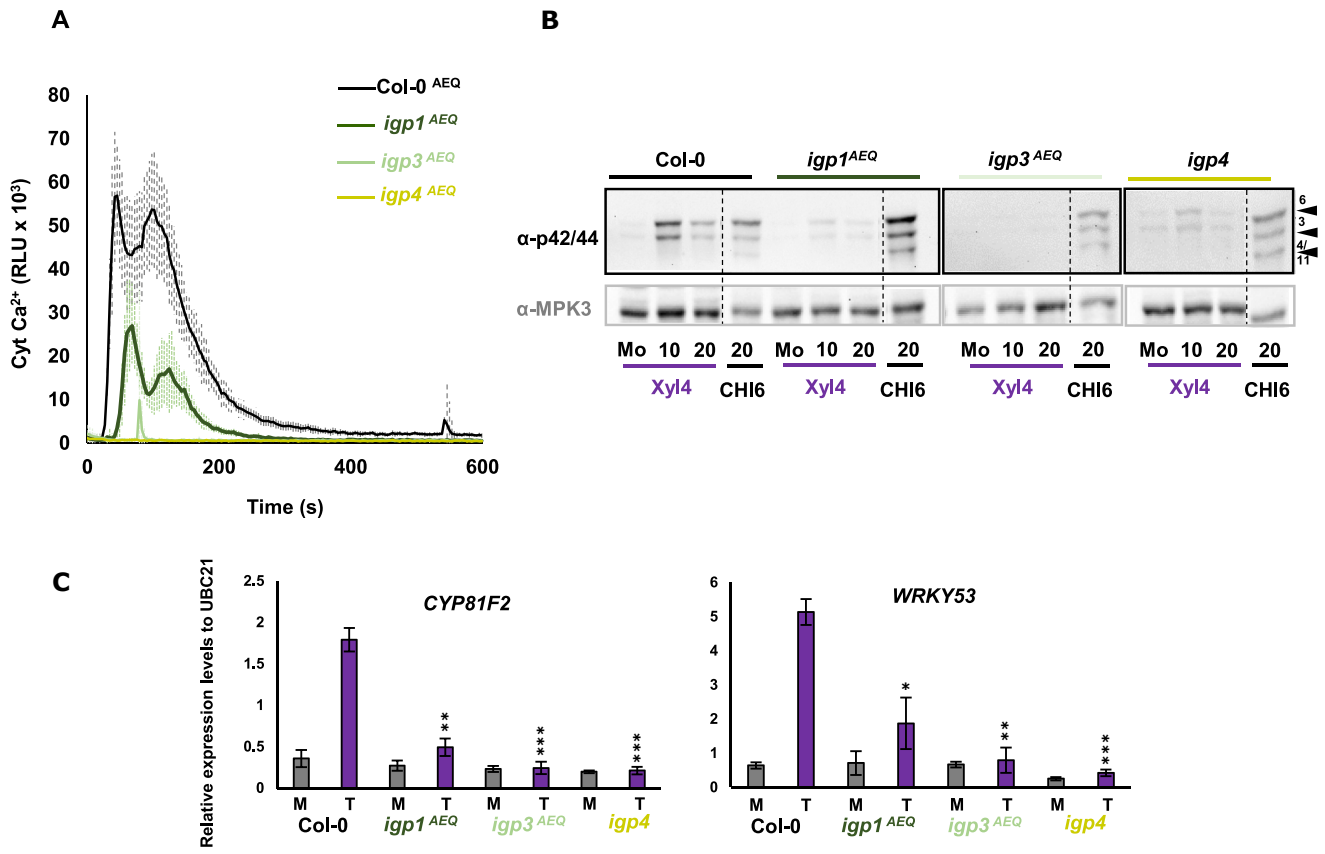

Fig. 3.

Fig. 3. *igp1, igp3 and igp4* mutants are impaired in XYL4 perception. The activation of immunity hallmarks such as cyt Ca^{2+} influx (A), phosphorylation of MPKs (B), and gene expression triggered by 250 μM XYL4 is defective in *igp* mutants tested. Experiments were performed as previously described in Fig. 1. Data represent (A) the mean ± error standard (n = 8) of two independent experiments performed, (B) a representative WB out of three replicates (dotted lines indicate that bands were cut from the membrane to relocate them in proper order), and (C) the mean ± error standard (n = 3) of three independent experiments. Statistically significant differences between compound-treated (T) plants versus mock-treated (M, H_2O) were calculated according to Student's *t*-test (*P < 0.05, **0.01 < P > 0.001, ***P < 0.001).

triggering ROS (Fig. 7). The activation of XYL4-triggered immune responses in *Arabidopsis thaliana*, tomato, and wheat suggests that these species have the receptors required for XYL4 perception and PTI activation and that xylan-derived oligosaccharides might be used for crop protection in tomato and other crops, as reported recently for mixtures of oligosaccharides derived from enzymatic hydrolysis of xylans (Pring et al., 2023).

Discussion

Activation of plant PTI by glycans derived from plant cell walls (DAMPs) and extracellular layers from pathogens (MAMPs) is an essential process to mount an effective disease resistance response during plant microbe-interactions (Bacete et al., 2018; Kongala and Kondreddy, 2023; Lee and Santiago, 2023). The structural diversity of glycans (DAMPs/MAMPs) that can be perceived by plants has been growing in the last years and include linear and branched oligosaccharides (generally of DP 3–10) which are mainly homo-oligosaccharides composed of D-monosaccharides (e.g. Glc, Xyl, Ara, GalA and Man) bound through different types of linkages (e.g. β-1,4, β-1,3, β-1,6 and α-1,4) (Klarzynski et al., 2000; Kaku et al., 2006; Aziz et al., 2007; Galletti et al., 2008; Claverie et al., 2018; Voxeur et al., 2019; Zang et al., 2019; Mélida et al., 2020; Malivert et al., 2021; Rebaque et al., 2021; Moussu et al., 2023; Pring et al., 2023). Also, branched oligosaccharides (e.g. with Ara at position 3 in XA_3XX or β-1,6-D-Glc branches in β-1,3-D-Glc glycans) have been shown to trigger PTI (Mélida et al., 2020; Wanke et al., 2020). These DAMPs/MAMPs can be released from plant cell walls and extracellular surfaces of microorganisms by the activity of CWDEs secreted by pathogens and plants during their interactions (Wanke et al., 2023). Thus, plant and microbial cell walls are rich sources of carbohydrate-based defence signalling molecules (DAMP and MAMPs) that are poorly characterized. Plant pathogens and their hosts have co-evolved an arsenal of CWDEs to break down the opponent's wall during their interactions (Rovenich et al., 2016). The great arsenal of CWDEs from pathogens and plants described (see CAZy database, www.cazy.org; (Drula et al., 2021)) and the huge diversity of polysaccharide structures present in plant walls (Delmer et al., 2024) and microorganism surfaces (Wanke et al., 2023) anticipate that the number of carbohydrate-based DAMPs/MAMPs recognized by plant immune system should grow significantly.

Here we show that *Arabidopsis thaliana* perceives β-1,4-D-XYL_4 further confirming previous results demonstrating that *Arabidopsis*

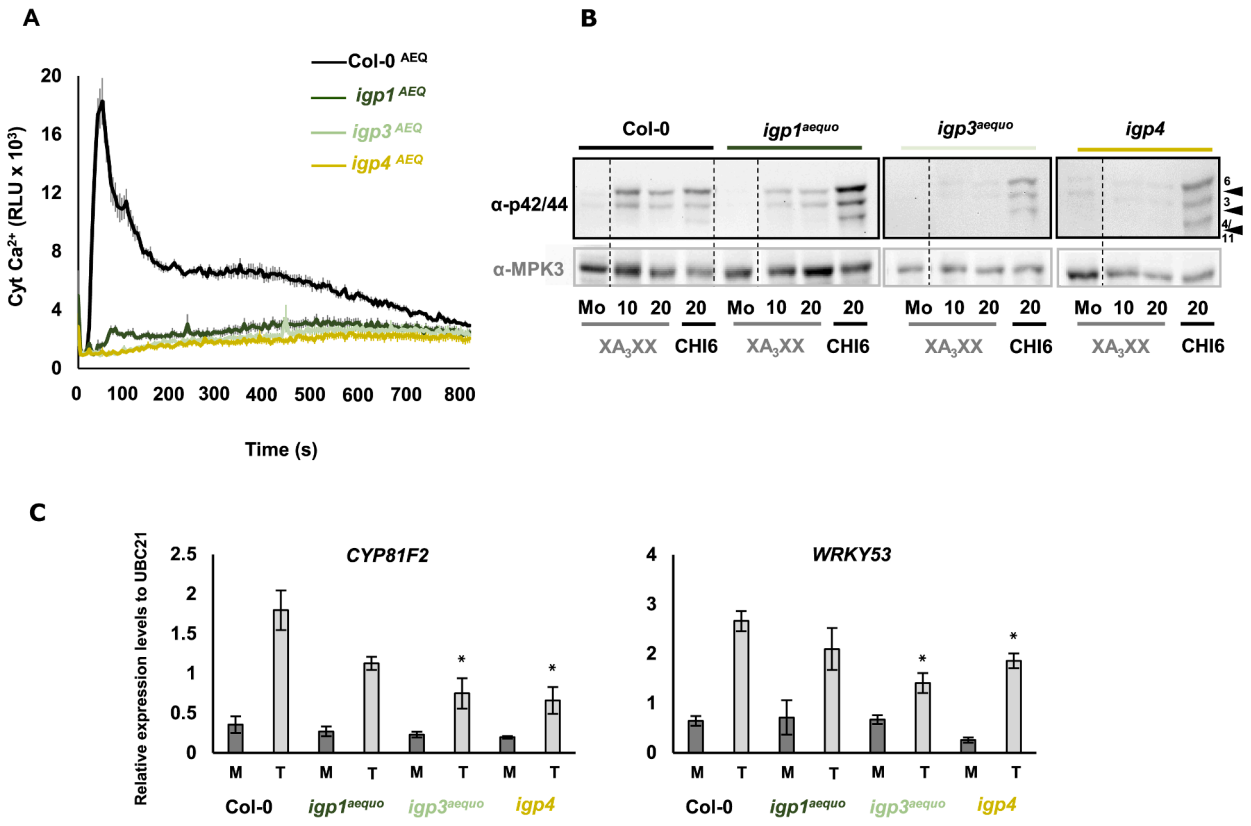

Fig. 4. *igp1, igp3 and igp4* mutants are impaired in XA_3XX perception. The activation of immunity hallmarks such as cyt Ca^{2+} influx (A) and phosphorylation of MPKs (B) is defective in *igp* mutants tested. Experiments were performed as described in Fig. 1. Data represent (A) the mean ± error standard (n = 8) of two independent experiments performed, (B) a representative WB out of three replicates (dotted lines indicate that bands were cut from the membrane to relocate them in proper order), and (C) the mean ± error standard (n = 3) of three independent experiments. Statistically significant differences between compound-treated (T) plants versus mock-treated (M, H2O) were calculated according to Student's *t*-test (*P < 0.05, **0.01 < P > 0.001, ***P < 0.001).

thaliana perceives oligosaccharides mixtures derived from xylan hydrolysis (Pring et al., 2023), including XYL2 disaccharide that triggers defensive-related responses and alteration in cell wall composition in *Arabidopsis thaliana* (Dewangan et al., 2023). We also show that *Arabidopsis thaliana* perceived previously undescribed plant-derived glycans like 2^3–(4-O-Methyl-α-D-Glucuronyl)-xylotetraose (XUXX) and α-glucans (α-1,4-D-Glc based maltodextrins: α-D-Maltotetraose (MAL4) and 6^3-α-D-Maltotriosyl-maltotriose ($MAL3_2$)), as well as polysaccharides mixtures from plants, like arabinogalactans (Fig. 1 and Fig. S2). The perception of XYL4 and XUXX by *Arabidopsis thaliana* immune system, together with the previous description of XA_3XX (Mélida et al., 2020), XYL2, XYL3 and XYL5 as DAMPs (Dewangan et al., 2023; Pring et al., 2023), suggest that linear and branched β-1,4-D-XYL_n oligosaccharides are perceived with different degree of specificity by plant immune systems. Notably, β-1,4-D-XYL_4 oligosaccharides with branching at position 2 show a reduced activity triggering PTI in comparison to XA_3XX which harbours an Ara at position 3 (Mélida et al., 2020). The observation that *Arabidopsis thaliana* recognizes β-1,6-D-Glc oligosaccharides (purified here for the first time from fungal pustulan), as well as fucoidan and low molecular weight-alginates (Figs. S1 and S2) is in line with the previous description of the effect of these compounds eliciting defensive and abiotic stress responses in different plant species (Aitouguinane et al., 2020; Aitouguinane et al., 2023; Liu et al., 2023), and indicates that their mechanisms of perception (e.g. PRRs) are conserved in *Arabidopsis thaliana*. Alginate is mainly composed of two conformational isomer residues, D-mannuronic acid (M) and L-guluronic acid (G), constituting homopolymeric (MM, GG) and heteropolymeric (MG, GM) sequential block structures (Aitouguinane et al., 2020; Aitouguinane et al., 2023). Fucoidans from brown marine algae are polysaccharides that consist predominantly of sulphated L-fucoses (Klarzynski et al., 2000; Wang et al., 2023). Our results and previous data indicate that *Arabidopsis thaliana* perceives glycan structures containing a great diversity of monosaccharides, including at least four different types of acidic monosaccharides (e.g. D-mannuronic acid and L-guluronic acid in alginates; Fig. S2), D-Glucuronyl in XUXX (Fig. 1) and GalA in OGs (Galletti et al., 2008; Voxeur et al., 2019; Liu et al., 2023). Also, *Arabidopsis thaliana* perceives glycan structures containing L-monosaccharides (L-Arabinose in arabinoxylans, L-Fucose in fucoidans and L-guluronic acid (G), in alginates: Fig. S2).

The molecular mechanisms implicated in the perception of glycans in plants are poorly characterized and just a few PRRs and co-PRRs have been described to be involved in these recognition processes. These PRRs characterised so far include LysM RKs (Kaku et al., 2006; Johnson et al., 2018; Yang et al., 2021a), members of the LRR-MAL, WAK, Malectin-like and Lectin RKs (Dai et al., 2023; Martín-Dacal et al., 2023; Moussu et al., 2023; Liu et al., 2024). However, with a few exceptions direct binding of glycans to ECDs of these RKs has not been demonstrated yet (Cao et al., 2014; Martín-Dacal et al., 2023). Here we showed that IGP1/CORK1, IGP3 and IGP4 proteins from LRR-MAL RK family, which are required for CEL3 and MLG43 perception and downstream PTI activation (Martín-Dacal et al., 2023), are also needed for the activation of immune responses triggered by XYL4 and XA_3XX, but not of other complex glycan structures, like fucoidan, alginates and arabinogalactans (Fig. 2 and Fig. S2). These results corroborate the relevance of this new family of LRR-MAL RKs as PRR/co-PRR in the activation of PTI in *Arabidopsis thaliana* and probably in other plant species (see Fig. 8).

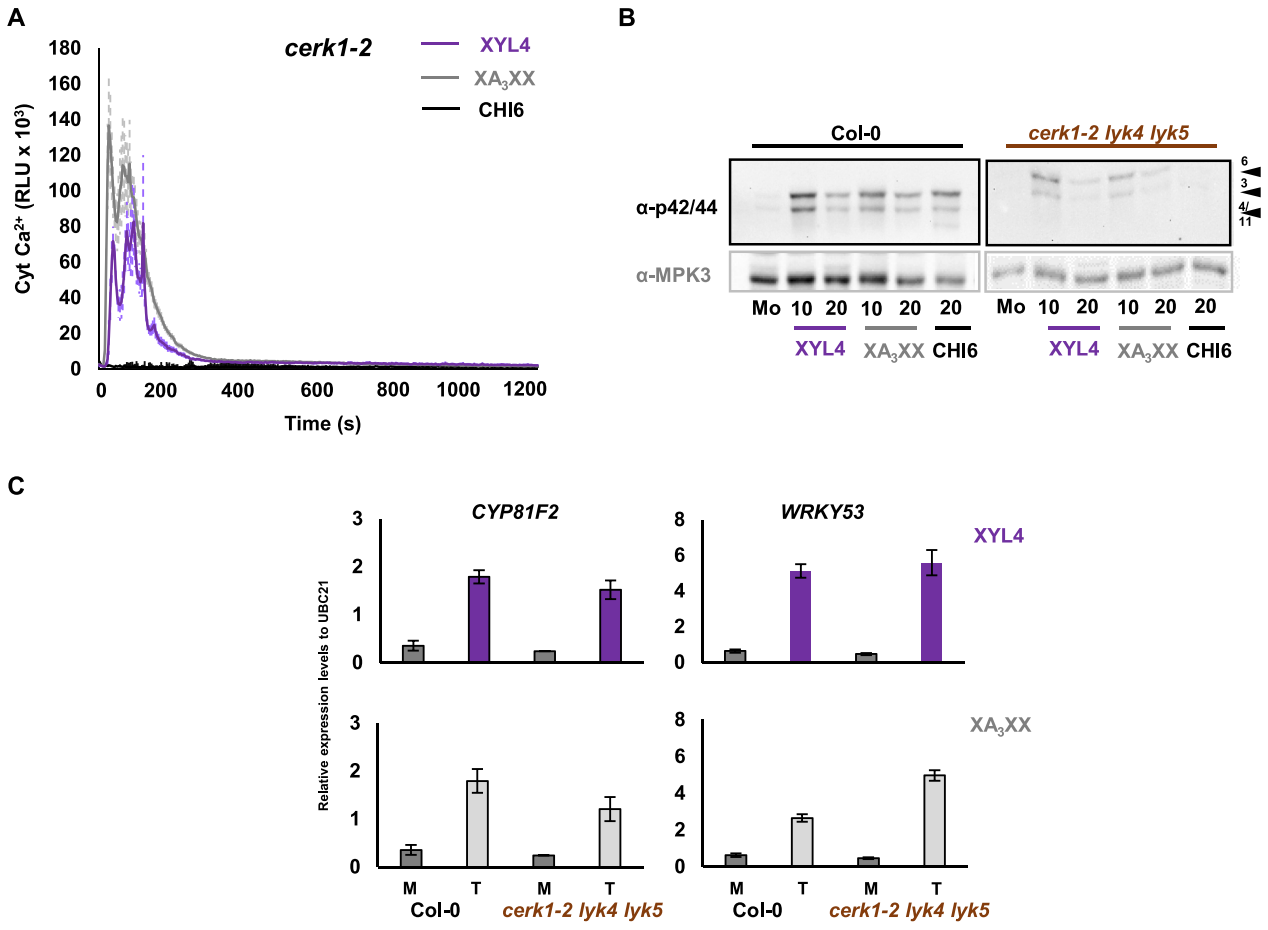

Fig. 5.

Fig. 5. CERK1, LYK4, and LYK5 LysM RKs have a minor role in XYL4 and XA_3XX perception. The activation of immunity hallmarks such as cyt Ca^{2+} influx (A) in *cerk1-2*^{AEQ} mutant line, and phosphorylation of MPKs (B) and gene marker expression (C) in *cerk1-2 lyk4 lyk5* triple mutant line are partially impaired after treatment with 450 μM of XYL4 or XA_3XX. Experiments were performed as previously described in Fig. 1. Data represent (A) the mean ± error standard (n = 8) of two independent experiments performed, (B) a representative WB out of three replicates (dotted lines indicate that bands were cut from the membrane to relocate them in proper order), and (C) the mean ± error standard (n = 3) of three independent experiments. Statistically significant differences between compound-treated (T) plants versus mock-treated (M, H_2O) were calculated according to Student's *t*-test (*P < 0.05, **0.01 < P > 0.001, ***P < 0.001).

Our data suggests that IGP RKs are central components in activation of immune responses (e.g. transcriptional upregulation of genes) triggered by a diversity of glycans with different carbohydrate moieties in their composition (Glc, Xyl, Ara) and distinct structures, that include, at least CEL3-CEL5, XYL4 and XA_3XX, as well as MLG43(Martín-Dacal et al., 2023)). These DAMPs can be released from plant cell wall polysaccharides by the action of microbial CWDEs (Fig. 8). Despite the differential composition and structures of these glycans, they share some features that might explain their similar mechanisms of perception by IGP1/IGP3/IGP4: i) they are composed of monosaccharides (pentose and hexoses) in pyranose conformation; and ii) they have two units bound with a β-1,4-D-linkage, including the anomeric carbon (position 1) that is probably in its reduced form. The differential impairment of PTI response upon XYL4 and XA_3XX observed in *igp4-1* and *igp3-1* (fully blocked responses), in comparison to *igp1-1* (partially impaired), might be explained by the fact that *igp1* is not a loss-of-function mutant, since a similar pattern of impairment of PTI responses has been observed after CEL3 and MLG43 treatment (Martín-Dacal et al., 2023). Whether IGP1/CORK1, IGP3 and IGP4 might be the *bona-fide* PRRs for XYL4 and XA_3XX require additional characterization and binding assays with their ECDs. Likewise, LRR-MAL RK family comprises 13 members in *Arabidopsis thaliana* and it cannot be excluded that some other additional RKs might be the *bona fide* PRRs for XYL4 and/or XA_3XX (Yang et al., 2021a; Martín-Dacal et al., 2023). Notably, LRR-MAL RK family members are present in all the plant species, including monocots, like wheat and rice, though the orthologs of IGP1/CORK1, IGP3 and IGP4 in other plant species have not been functionally characterized (Yang et al., 2021b; Martin-Dacal et al., 2023). Though some of these LRR-MAL RK members have been involved in pollen migration and fertility (Lee et al., 2024), an alternative function for such PRRs in oligosaccharide perception cannot be discarded, since pollen migration and lateral root formation promote changes in cell wall integrity and composition (Moussu et al., 2023; Lee et al., 2024). Despite the relevance of LRR-MAL RKs in glycan perception and PTI activation, additional, uncharacterized mechanisms for oligosaccharide recognition should exist in *Arabidopsis thaliana*, because the perception of glycans present in arabinogalactan proteins and seaweed glycans triggering defensive responses (i.e., fucoidan and alginates) is not altered in *igp1/cork1* and *igp4* mutants (Fig. S2).

Here we also showed that the mechanisms of perception of XYL4 and XA_3XX might require the LysM-RKs CERK1, LYK5 and LYK4, probably

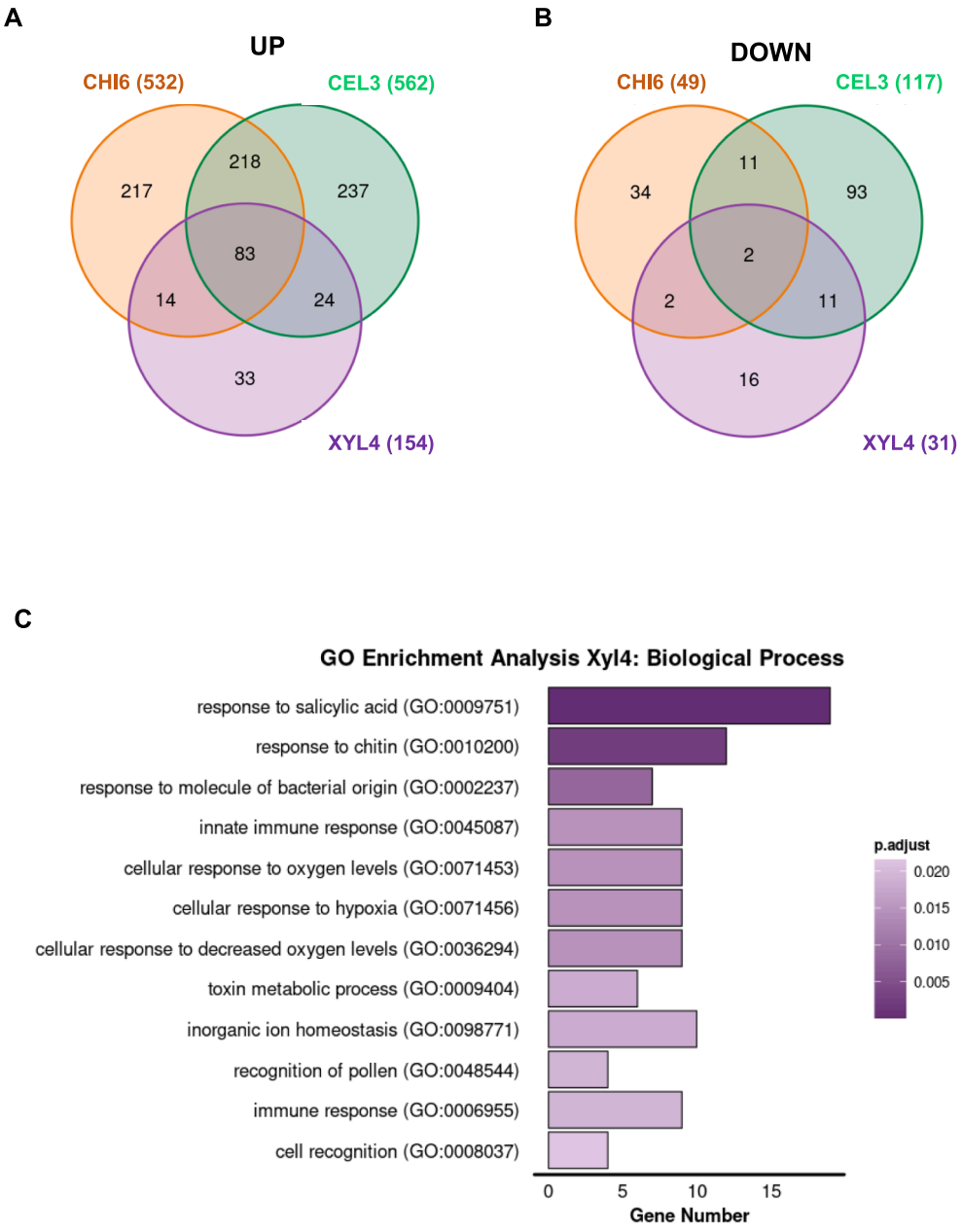

Fig. 6.

Fig. 6. XYL4 triggers the differential regulation of immunity-associated genes in *Arabidopsis thaliana*. (A)Venn diagrams of the number of the differentially expressed genes (DEGs) up-regulated (left) and down-regulated (right) upon treatment of *Arabidopsis thaliana* Col-0 seedlings with either XYL4 (250 μM), CEL3 (50 μM) or CHI6 (50 μM). The total number of DEGs is indicated with the glycan and the overlapped genes are shown in the circles. (B) GO enrichment analysis of biological process among the up DEGs upon treatment with XYL4. See material and methods for additional details.

acting as redundant co-receptors. These LysM-RKs, which are required for CHI6 perception and PTI activation (Fig. 8), have been shown to function as putative co-receptors for MLG43 and β-1,3-Glc oligosaccharides (e.g. LAM6) (Mélida et al., 2018; del Hierro et al., 2021; Rebaque et al., 2021). Notably, perception of CHI6, that can be released from fungal cell wall by the action of plant CWDEs, does not requires IGP1/CORK1, IGP3 or IGP4 RKs, indicating that these sets of receptors (LysM-RKs and LRR-MAL RKs) control different PTI signalling pathways (Fig. 8). PTI responses triggered by CHI6 and XYL4 are shown here to activate transcriptional responses that share over 80 % of the up-regulated genes, further demonstrating a very high gene reprogramming overlap upon treatment with these glyco-ligands (Figs. 6 and 8). These data are in line with previous transcriptomic analyses comparing *Arabidopsis thaliana* responsive genes to single-linked β-1,3- (DAMP/MAMP) and β-1,4-glucans (DAMPs) and chitin (MAMP) that revealed that a significant percentage of DEGs were common between glucans

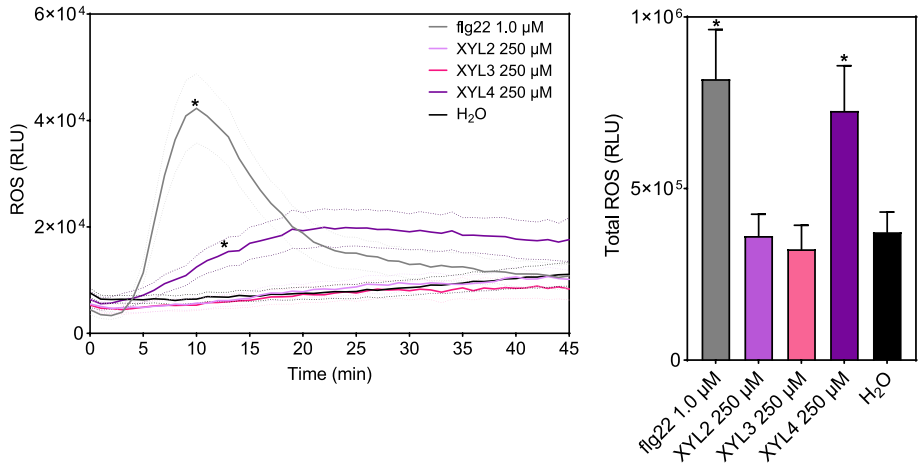

Fig. 7.

Fig. 7. XYL4 activates ROS production in wheat·H_2O_2 accumulation in wheat leaves of cultivar Titlis upon treatment with 250 μM of XYL2, XYL3, or XYL4·H_2O_2 levels were estimated by measuring for 45 min the relative luminescence units (RLU) using the luminol-20 assay. The peptide flg22 (1 μM) and H_2O were used as positive and negative controls, respectively. The total ROS production is displayed on the right side of the panel. The standard error of the mean (n = 8) is shown. Asterisks (*) indicate significant differences (*$p < 0.05$) with the negative control according to the Kruskal-Wallis test. This is one of the three experiments performed with similar results.

and chitin treatments (Souza et al., 2017; Johnson et al., 2018; Mélida et al., 2018).

As previously described for XA_3XX (Mélida et al., 2020), we show here that XYL4 is perceived by different plant species (tomato and wheat) and that pre-treatment of these species with XYL4 triggers PTI responses (i.e. in wheat; Fig. 7) and crop protection (i.e. in tomato; Fig. 4S). These data support that LRR-MAL RK orthologs of IGP1/CORK1, IGP3 and IGP4 are present in other plant species, including wheat and tomato, that deserve further characterization (Yang et al., 2021b; Martin-Dacal et al., 2023). These data are also in line with the recent demonstration of the activity of mixtures of oligosaccharides from xylan hydrolysis on crop protection (Dewangan et al., 2023; Pring et al., 2023). Similarly, several studies have reported the use of alginate in agriculture to stimulate plant growth and development (Liu et al., 2023) and to induce plant resistance mechanisms, but the molecular bases of these responses have not been determined (Klarzynski et al., 2000; Aitouguinane et al., 2020; Aitouguinane et al., 2023; Wang et al., 2023). Together these results confirm the potential of glycans to activate PTI and to develop biological products that boost crop natural defence against pathogens, contributing to replacing chemical pesticides and implementing more sustainable agriculture practices. In the last years, several glycan-based agrobiological products have been successfully developed to be used in agriculture (e.g. products based on cell walls/extracts of brown Seaweed, laminarin, or chitin). However, the identification of active glycans in these complex mixtures and the determination of their mechanism of perception (e.g. identification of PRRs) by crops is essential to further expand a glycańs science-based technology in agriculture.

Funding and Acknowledgements

This work was supported by grants RTI2018-096975-B-I00 to AM funded by Spanish Ministry of Science, Innovation and Universities, and by grant PID2021-126006OB-I00 to AM, funded by MCIN/AEI/ https://doi.org/10.13039/501100011033 and by "ERDF A way of making Europe". This work was also supported by ĹOreal-FWIS Spanish edition 2019 grant to PF-C "*Inmunidad por azúcares en plantas*". PF-C, HM and CCL have been financially supported by the "Severo Ochoa Program for Centres of Excellence in R&D (grant SEV-2016-0672 and CEX2020-000999-S (2022-2025)) funded by MCIN/AEI/ https://doi.org/10.13039/501100011033. MA was a postdoctoral fellow supported by PID2021-126006OB-I00. MM-D was the recipient of PhD fellow (PRE2019-08812). ASV was a recipient of the RYC2018-025530-I grant from the Spanish Ministry of Science, Innovation, and Universities. SG-B was supported by PTA2021-020636-I, funded by the Spanish Ministry of Science and Innovation (MCIN/AEI/https://dx.https://doi.org/10.13039/501100011033) and the European Social Fund Plus (FSE+).

We thank Lucia Jordá and Miguel Ángel Torres for the critical reading of the manuscript and suggestions provided.

CRediT authorship contribution statement

Patricia Fernández-Calvo: Writing – original draft, Validation, Supervision, Investigation, Funding acquisition, Formal analysis, Data curation, Conceptualization. **Gemma López:** Methodology, Investigation, Formal analysis. **Marina Martín-Dacal:** Validation, Methodology, Investigation, Formal analysis, Data curation. **Meriem Aitouguinane:** Validation, Methodology, Investigation, Formal analysis. **Cristian Carrasco-López:** Writing – original draft, Validation, Methodology, Investigation, Formal analysis. **Sara González-Bodí:** Writing – original draft, Software, Methodology, Investigation, Formal analysis, Data curation. **Laura Bacete:** Methodology, Investigation, Formal analysis. **Hugo Mélida:** Writing – original draft, Validation, Supervision, Methodology, Investigation, Formal analysis, Conceptualization. **Andrea Sánchez-Vallet:** Writing – original draft, Investigation, Formal analysis, Conceptualization. **Antonio Molina:** Writing – original draft, Validation, Supervision, Project administration, Methodology, Investigation, Funding acquisition, Formal analysis, Data curation, Conceptualization.

Declaration of competing interest

The authors declare the following financial interests/personal relationships which may be considered as potential competing interests: Antonio Molina reports financial support was provided by Spanish Research Agency. Patricia Fernandez-Calvo reports financial support

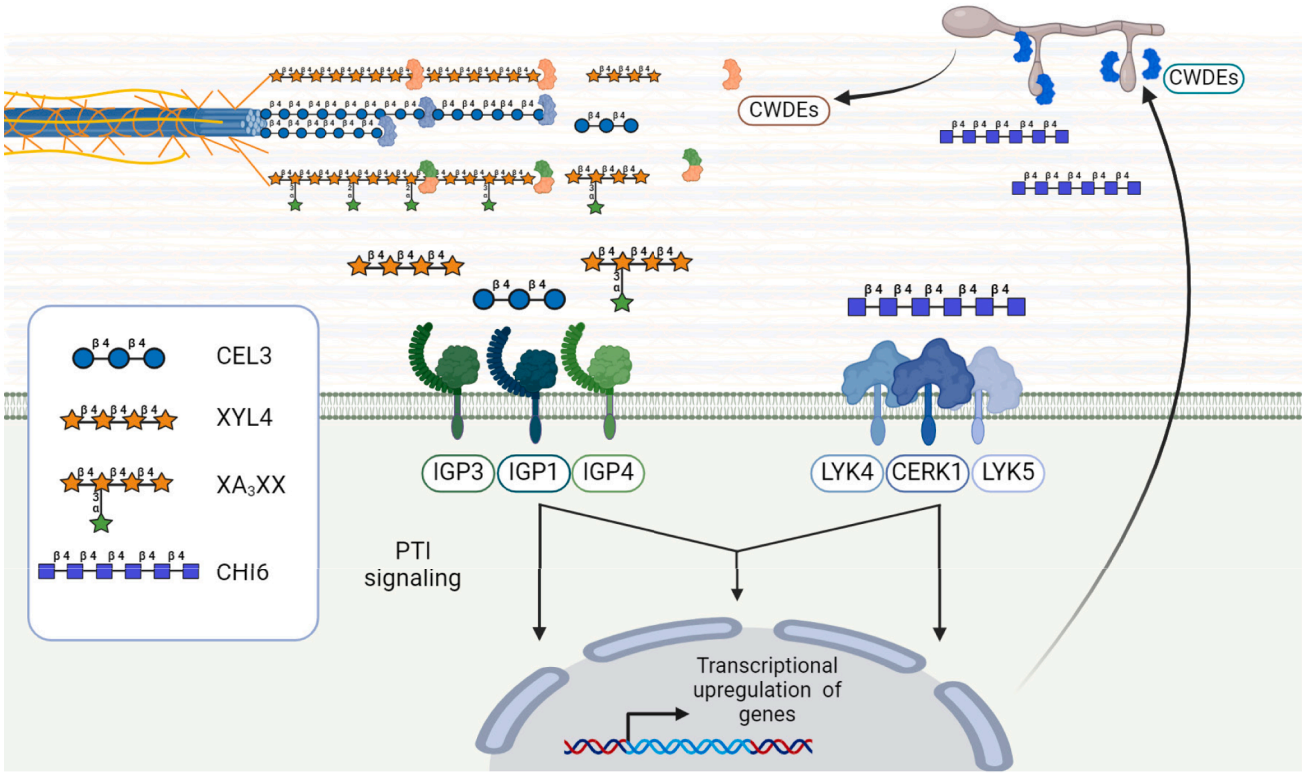

Fig. 8.

Fig. 8. Model of IGPs function in the perception of glycans with different composition. Fungi secretes CWDEs that hydrolyse plant cell wall polysaccharides (cellulose, xylans and arabinoxylans) releasing DAMPs like XYL4, XA_3XX or CEL3 that are perceived through LRR-MAL RKs (IGP1/CORK1, IGP3 and IGP4) triggering PTI and transcriptional upregulation of genes. Plants can secrete CWDEs that hydrolyse chitin from fungal cell walls releasing CHI6 MAMPs that is perceived through LysM-RKs (CERK1, LYK5 and LYK4) triggering PTI responses, which overlap with some PTI responses triggered by IGPs RKs.

was provided by L óreal Spain. Patricia Fernandez-Calvo reports was provided by Spanish Research Agency. Hugo Melida reports financial support was provided by Spanish Research Agency. Marina Martin-Dacal reports financial support was provided by Spanish Research Agency. Cristian Carrasco-Lopez reports financial support was provided by Spanish Research Agency. Sara Gonzalez-Bodi reports financial support was provided by Spanish Research Agency. If there are other authors, they declare that they have no known competing financial interests or personal relationships that could have appeared to influence the work reported in this paper.

Appendix A. Supplementary data

Supplementary data to this article can be found online at https://doi.org/10.1016/j.tcsw.2024.100124.

References

Aitouguinane, M., Bouissil, S., Mouhoub, A., Rchid, H., Fendri, I., Abdelkafi, S., Ould El-Hadj, M.D., Boual, Z., Dubessay, P., Gardarin, C., Michaud, P., El Alaoui-Talibi, Z., El Modafar, C., Pierre, G., Delattre, C., 2020. Induction of natural defenses in tomato seedlings by using alginate and oligoalginates derivatives Extracted from moroccan Brown algae. Mar. Drugs 18, 521.

Aitouguinane, M., El Alaoui-Talibi, Z., Rchid, H., Fendri, I., Abdelkafi, S., El-Hadj, M.D. O., Boual, Z., Le Cerf, D., Rihouey, C., Gardarin, C., Dubessay, P., Michaud, P., Pierre, G., Delattre, C., El Modafar, C., 2023. Elicitor activity of low-Molecular-weight alginates obtained by oxidative degradation of alginates Extracted from Sargassum muticum and Cystoseira myriophylloides. Mar. Drugs 21.

Anders S, Pyl PT, Huber W (2010) HTSeq: Analysing high-throughput sequencing data with Python.

Andrews, S., 2010. FastQC: A Quality Control Tool for High Throughput Sequence Data. In.

Aziz, A., Gauthier, A., Bézier, A., Poinssot, B., Joubert, J.M., Pugin, A., Heyraud, A., Baillieul, F., 2007. Elicitor and resistance-inducing activities of beta-1,4 cellodextrins in grapevine, comparison with beta-1,3 glucans and alpha-1,4 oligogalacturonides. J. Exp. Bot. 58, 1463–1472.

Bacete, L., Mélida, H., Pattathil, S., Hahn, M.G., Molina, A., Miedes, E., 2017. Characterization of plant Cell Wall damage-associated Molecular patterns regulating immune responses. Methods Mol. Biol. 1578, 13–23.

Bacete, L., Mélida, H., Miedes, E., Molina, A., 2018. Plant cell wall-mediated immunity: cell wall changes trigger disease resistance responses. Plant J. 93, 614–636.

Benkeblia, N., 2020. Potato glycoalkaloids: occurrence, biological activities and extraction for biovalorisation – a review. Int. J. Food Sci. Technol. 55, 8.

Bigeard, J., Colcombet, J., Hirt, H., 2015. Signaling mechanisms in pattern-triggered immunity (PTI). Mol. Plant 8, 521–539.

Bolger, A., Marc, L., Bjoern, U., 2014. Trimmomatic: a flexible trimmer for illumina sequence data. Bioinformatics 30.

Bordeleau, S.J., Canales Sanchez, L.E., Goring, D.R., 2022. Finding new Arabidopsis receptor kinases that regulate compatible pollen-pistil interactions. Front. Plant Sci. 13.

Boutrot, F., Zipfel, C., 2017. Function, discovery, and exploitation of plant pattern recognition receptors for broad-Spectrum disease resistance. Annu. Rev. Phytopathol. 55, 257–286.

Cao, Y., Liang, Y., Tanaka, K., 2014. The kinase LYK5 is a major chitin receptor in Arabidopsis and forms a chitin-induced complex with related kinase CERK1. Elife 3.

Chandrasekar, B., Wanke, A., Wawra, S., Saake, P., Mahdi, L., Charura, N., Neidert, M., Poschmann, G., Malisic, M., Thiele, M., Stühler, K., Dama, M., Pauly, M., Zuccaro, A., 2022. Fungi hijack a ubiquitous plant apoplastic endoglucanase to release a ROS scavenging β-glucan decasaccharide to subvert immune responses. Plant Cell 34, 19.

Cheng, C.Y., Krishnakumar, V., Chan, A.P., Thibaud-Nissen, F., Schobel, S., Town, C.D., 2017. Araport11: a complete reannotation of the Arabidopsis thaliana reference genome. Plant J. 89, 789–804.
Claverie, J., Balacey, S., Lemaitre-Guillier, C., Brule, D., Chiltz, A., Granet, L., Noirot, E., Daire, X., Darblade, B., Heloir, M.C., Poinssot, B., 2018. The Cell Wall-derived xyloglucan is a new DAMP triggering plant immunity in Vitis vinifera and Arabidopsis thaliana. Front. Plant Sci. 9, 1725.
Dai, Y.-S., Liu, D., Guo, W., Liu, Z.-X., Zhang, X., Shi, L.-L., Zhou, D.-M., Wang, L.-N., Kang, K., Wang, F.-Z., Zhao, S.-S., Tan, Y.-F., Hu, T., Chen, W., Li, P., Zhou, Q.-M., Yuan, L.-Y., Zhang, Z., Chen, Y.-Q., Zhang, W.-Q., Li, J., Yu, L.-J., Xiao, S., 2023. Poaceae-specific β-1,3;1,4-d-glucans link jasmonate signalling to OsLecRK1-mediated defence response during rice-brown planthopper interactions. Plant Biotechnol. J. 21, 1286–1300.
del Hierro, I., Mélida, H., Broyart, C., Santiago, J., Molina, A., 2021. Computational prediction method to decipher receptor–glycoligand interactions in plant immunity. Plant J. 105, 1710–1726.
Delmer, D., Dixon, R.A., Keegstra, K., Mohnen, D., 2024. The plant cell wall—dynamic, strong, and adaptable—is a natural shapeshifter. Plant Cell. https://doi.org/10.1093/pcell/koad325.
Desaki, Y., Kouzai, Y., Ninomiya, Y., Iwase, R., Shimizu, Y., Seko, K., Molinaro, A., Minami, E., Shibuya, N., Kaku, H., Nishizawa, Y., 2018. OsCERK1 plays a crucial role in the lipopolysaccharide-induced immune response of rice. New Phytol. 217, 1042–1049.
Dewangan, B.P., Gupta, A., Sah, R.K., Das, S., Kumar, S., Bhattacharjee, S., Pawar, P.-A.-M., 2023. Xylobiose treatment triggers a defense-related response and alters cell wall composition. Plant Mol. Biol. 113, 383–400.
Dobin, A., Davis, C.A., Schlesinger, F., Drenkow, J., Zaleski, C., Jha, S., Batut, P., Chaisson, M., Gingeras, T.R., 2013. STAR: ultrafast universal RNA-seq aligner. Bioinformatics 29, 15–21.
Dobrange, E., Peshev, D., Loedolff, B., Van den Ende, W., 2019. Fructans as immunomodulatory and antiviral agents: the case of echinacea. Biomolecules 9.
Drula, E., Garron, M.-L., Dogan, S., Lombard, V., Henrissat, B., Terrapon, N., 2021. The carbohydrate-active enzyme database: functions and literature. Nucleic Acids Res. 50, D571–D577.
Ewels, P., Magnusson, M., Lundin, S., Kaller, M., 2016. MultiQC: summarize analysis results for multiple tools and samples in a single report. Bioinformatics 32, 3047–3048.
Galletti, R., Denoux, C., Gambetta, S., Dewdney, J., Ausubel, F.M., De Lorenzo, G., Ferrari, S., 2008. The AtrbohD-mediated oxidative burst elicited by oligogalacturonides in Arabidopsis is dispensable for the activation of defense responses effective against Botrytis cinerea. Plant Physiol. 148, 1695–1706.
Gómez-Gómez, L., Boller, T., 2000. FLS2: an LRR receptor-like kinase involved in the perception of the bacterial elicitor flagellin in Arabidopsis. Mol. Cell 5, 1003–1011.
Gust, A.A., Biswas, R., Lenz, H.D., Rauhut, T., Ranf, S., Kemmerling, B., Götz, F., Glawischnig, E., Lee, J., Felix, G., Nürnberger, T., 2007. Bacteria-derived peptidoglycans constitute pathogen-associated molecular patterns triggering innate immunity in Arabidopsis. J. Biol. Chem. 282, 32338–32348.
Hou, S., Liu, Z., Shen, H., Wu, D., 2019. Damage-associated Molecular pattern-triggered immunity in plants. Front. Plant Sci. 22, 646.
Johnson, J.M., Thürich, J., Petutschnig, E.K., Altschmied, L., Meichsner, D., Sherameti, I., Dindas, J., Mrozinska, A., Paetz, C., Scholz, S.S., Furch, A.C.U., Lipka, V., Hedrich, R., Schneider, B., Svatoš, A., Oelmüller, R., 2018. A poly(a) ribonuclease controls the cellotriose-based Interaction between piriformospora indica and its host Arabidopsis. Plant Physiol. 176, 2496–2514.
Kaku, H., Nishizawa, Y., Ishii-Minami, N., Akimoto-Tomiyama, C., Dohmae, N., Takio, K., Minami, E., Shibuya, N., 2006. Plant cells recognize chitin fragments for defense signaling through a plasma membrane receptor. PNAS 103, 11086–11091.
Kemmerling, B., Schwedt, A., Rodriguez, P., Mazzotta, S., Frank, M., Qamar, S.A., Mengiste, T., Betsuyaku, S., Parker, J.E., Müssig, C., Thomma, B.P., Albrecht, C., de Vries, S.C., Hirt, H.T.N., 2007. The BRI1-associated kinase 1, BAK1, has a brassinolide-independent role in plant cell-death control. Curr. Biol. 17.
Klarzynski, O., Plesse, B., Joubert, J.M., Yvin, J.C., Kopp, M., Kloareg, B., Fritig, B., 2000. Linear beta-1,3 glucans are elicitors of defense responses in tobacco. Plant Physiol. 124, 1027–1038.
Knight, M.R., Campbell, A.K., Smith, S.M., Trewavas, A.J., 1991. Transgenic plant aequorin reports the effects of touch and cold-shock and elicitors on cytoplasmic calcium. Nature 352, 524–526.
Kongala, S.I., Kondreddy, A., 2023. A review on plant and pathogen derived carbohydrates, oligosaccharides and their role in plant's immunity. Carbohydrate Polymer Technologies and Applications 6, 100330.
Kraemer, F.J., Lunde, C., Koch, M., Kuhn, B.M., Ruehl, C., Brown, P.J., Hoffmann, P., Göhre, V., Hake, S., Pauly, M., Ramírez, V., 2021. A mixed-linkage (1,3;1,4)-β-D-glucan specific hydrolase mediates dark-triggered degradation of this plant cell wall polysaccharide. Plant Physiol. 185, 1559–1573.
Lee, H.K., Canales Sanchez, L.E., Bordeleau, S.J., Goring, D.R., 2024. Arabidopsis leucine-rich repeat malectin receptor–like kinases regulate pollen–stigma interactions. Plant Physiol.
Lee, H.K., Santiago, J., 2023. Structural insights of cell wall integrity signaling during development and immunity. Curr. Opin. Plant Biol. 76, 102455.
Liu, J., Li, W., Wu, G., Ali, K., 2024. An update on evolutionary, structural, and functional studies of receptor-like kinases in plants. Front. Plant Sci. 15.
Liu, T., Liu, Z., Song, C., Hu, Y., Han, Z., She, J., Fan, F., Wang, J., Jin, C., Chang, J., Zhou, J.M., Chai, J., 2012. Chitin-induced dimerization activates a plant immune receptor. Science 336, 1160–1164.
Liu, S., Wang, Q., Shao, Z., Liu, Q., He, Y., Ren, D., Yang, H., Li, X., 2023. Purification and Characterization of the enzyme fucoidanase from cobetia amphilecti utilizing fucoidan from Undaria pinnatifida. Foods 12, 1555.
Love, M., Wolfgang, H., Simon, A., 2014. Moderated estimation of fold change and dispersion for RNA-seq data with DESeq2. Genome Biol. 15.
Ma, Chaube, Trattnig, N., Lee, D.H., Belkhadir, Y., Pfrengle, F., 2022. Synthesis of Fungal Cell Wall Oligosaccharides and Their Ability to Trigger Plant Immune Responses. Eur. J. Org. Chem. e202200313.
Malivert, A., Erguvan, O., Chevallier, A., Dehem, A., Friaud, R., Liu, M., Martin, M., Peyraud, T., Hamant, O., Verger, S., 2021. FERONIA and microtubules independently contribute to mechanical integrity in the Arabidopsis shoot. PLoS Biol. 19, e3001454.
Martín-Dacal, M., Fernández-Calvo, P., Jiménez-Sandoval, P., López, G., Garrido-Arandía, M., Rebaque, D., del Hierro, I., Berlanga, D.J., Torres, M.Á., Kumar, V., Mélida, H., Pacios, L.F., Santiago, J., Molina, A., 2023. Arabidopsis immune responses triggered by cellulose- and mixed-linked glucan-derived oligosaccharides require a group of leucine-rich repeat malectin receptor kinases. Plant J. 113, 833–850.
Mélida, H., Sopeña-Torres, S., Bacete, L., Garrido-Arandia, M., Jordá, L., López, G., Muñoz-Barrios, A., Pacios, L.F., Molina, A., 2018. Non-branched β-1,3-glucan oligosaccharides trigger immune responses in Arabidopsis. Plant J. 93, 34–49.
Mélida, H., Bacete, L., Ruprecht, C., Rebaque, D., Del Hierro, I., López, G., Brunner, F., Pfrengle, F., Molina, A., 2020. Arabinoxylan-Oligosaccharides act as damage associated Molecular patterns in plants regulating disease resistance. Front. Plant Sci. 11, 1210.
Miya, A., Albert, P., Shinya, T., Desaki, Y., Ichimura, K., Shirasu, K., Narusaka, Y., Kawakami, N., Kaku, H., Shibuya, N., 2007. CERK1, a LysM receptor kinase, is essential for chitin elicitor signaling in Arabidopsis. PNAS 104, 19613–19618.
Moussu, S., Lee, H.K., Haas, K.T., Broyart, C., Rathgeb, U., De Bellis, D., Levasseur, T., Schoenaers, S., Fernandez, G.S., Grossniklaus, U., Bonnin, E., Hosy, E., Vissenberg, K., Geldner, N., Cathala, B., Höfte, H., Santiago, J., 2023. Plant cell wall patterning and expansion mediated by protein-peptide-polysaccharide interaction. Science 382, 719–725.
Ngou, B.P.M., Ding, P., Jones, J.D.G., 2022. Thirty years of resistance: zig-zag through the plant immune system. Plant Cell 34, 1447–1478.
Nguyen, Q.M., Iswanto, A.B.B., Son, G.H., Kim, S.H., 2021. Recent advances in effector-triggered immunity in plants: new pieces in the puzzle create a different Paradigm. Int. J. Mol. Sci. 22.
Pring, S., Kato, H., Imano, S., Camagna, M., Tanaka, A., Kimoto, H., Chen, P., Shrotri, A., Kobayashi, H., Fukuoka, A., Saito, M., Suzuki, T., Terauchi, R., Sato, I., Chiba, S., Takemoto, D., 2023. Induction of plant disease resistance by mixed oligosaccharide elicitors prepared from plant cell wall and crustacean shells. Physiol. Plant. 175, e14052.
Ranf, S., Grimmer, J., Pöschl, Y., Pecher, P., Chinchilla, D., Scheel, D., Lee, J., 2012. Defense-related calcium signaling mutants uncovered via a quantitative high-throughput screen in Arabidopsis thaliana. Mol. Plant 5, 115–130.
Rebaque, D., del Hierro, I., López, G., Bacete, L., Vilaplana, F., Dallabernardina, P., Pfrengle, F., Jordá, L., Sánchez-Vallet, A., Pérez, R., Brunner, F., Molina, A., Mélida, H., 2021. Cell wall-derived mixed-linked β-1,3/1,4-glucans trigger immune responses and disease resistance in plants. Plant J. 106, 601–615.
Rovenich, H., Zuccaro, A., Thomma, B.P., 2016. Convergent Evolution of Filamentous Microbes towards Evasion of Glycan-Triggered Immunity 212, 896–901.
Santamaría-Hernando, S., Senovilla, M., González-Mula, A., Martínez-García, P.M., Nebreda, S., Rodríguez-Palenzuela, P., López-Solanilla, E., Rodríguez-Herva, J.J., 2019. The Pseudomonas syringae pv. tomato DC3000 PSPTO_0820 multidrug transporter is involved in resistance to plant antimicrobials and bacterial survival during tomato plant infection. PLoS One 14, e0218815.
Souza, C.A., Li, S., Lin, A.Z., 2017. Cellulose-derived Oligomers act as damage-associated Molecular patterns and trigger defense-like responses. Plant Physiol. 173, 2383–2398.
Tanaka, K., Heil, M., 2021. Damage-associated Molecular patterns (DAMPs) in plant innate immunity: applying the danger model and Evolutionary perspectives. Annu. Rev. Phytopathol. 59, 18.
Tang, D., Wang, G., 2017. Receptor kinases in plant-pathogen Interactions: more than pattern recognition. Plant Cell 29, 618–637.
Tseng, Y.-H., Scholz, S.S., Fliegmann, J., Krüger, T., Gandhi, A., Furch, A.C.U., Kniemeyer, O., Brakhage, A.A., Oelmüller, R., 2022. CORK1, a LRR-malectin receptor kinase, is required for Cellooligomer-induced responses in Arabidopsis thaliana. Cells 11, 2960.
Voxeur, A., Habrylo, O., Guénin, S., Miart, F., Soulié, M.C., Rihouey, C., Pau-Roblot, C., Domon, J.M., Gutierrez, L., Pelloux, J., 2019. Oligogalacturonide production upon Arabidopsis thaliana-Botrytis cinerea interaction. PNAS 116, 19743–19752.
Wang, M., Veeraperumal, S., Zhong, S., Cheong, K.L., 2023. Fucoidan-derived functional Oligosaccharides: recent developments, preparation, and potential applications. Foods 12.
Wanke, A., Rovenich, H., Schwanke, F., Velte, S., Becker, S., Hehemann, J.H., Wawra, S., Zuccaro, A., 2020. Plant species-specific recognition of long and short β-1,3-linked glucans is mediated by different receptor systems. Plant J. 102, 1142–1156.
Wanke, A., van Boerdonk, S., Mahdi, L.K., Wawra, S., Neidert, M., Chandrasekar, B., Saake, P., Saur, I.M.L., Derbyshire, P., Holton, N., Menke, F.L.H., Brands, M., Pauly, M., Acosta, I.F., Zipfel, C., Zuccaro, A., 2023. A GH81-type β-glucan-binding protein enhances colonization by mutualistic fungi in barley. Curr. Biol. 33, 5071–5084.e5077.
Wickham H (2016) ggplot2 Elegant Graphics for Data Analysis. In S link, ed, Springer International Publishing, Ed Second Edition.

Willmann, R., Lajunen, H.M., Erbs, G., Newman, M.A., Kolb, D., Tsuda, K., Katagiri, F., Fliegmann, J., Bono, J.J., Cullimore, J.V., Jehle, A.K., Götz, F., Kulik, A., Molinaro, A., Lipka, V., Gust, A.A., Nürnberger, T., 2011. Arabidopsis lysin-motif proteins LYM1 LYM3 CERK1 mediate bacterial peptidoglycan sensing and immunity to bacterial infection. PNAS 108, 19824–19829.

Wu, T., Hu, E., Xu, S., Chen, M., Guo, P., Dai, Z., Feng, T., Zhou, L., Tang, W., Zhan, L., Fu, X., Liu, S., Bo, X., Yu, G., 2021. clusterProfiler 4.0: a universal enrichment tool for interpreting omics data. Innovation (Camb.) 2, 100141.

Yang, C., Liu, R., Pang, J., Ren, B., Zhou, H., Wang, G., Wang, E., Liu, J., 2021a. Poaceae-specific cell wall-derived oligosaccharides activate plant immunity via OsCERK1 during magnaporthe oryzae infection in rice. Nat. Commun. 12, 2178.

Yang, H., Wang, D., Guo, L., Pan, H., Yvon, R., Garman, S., Wu, H.-M., Cheung, A.Y., 2021b. Malectin/Malectin-like domain-containing proteins: a repertoire of cell surface molecules with broad functional potential. Cell Surface 7, 100056.

Yuan, M., Ngou, B.P.M., Ding, P., Xin, X.F., 2021. PTI-ETI crosstalk: an integrative view of plant immunity. Curr. Opin. Plant Biol. 62, 102030.

Zang, H., Xie, S., Zhu, B., Yang, X., Gu, C., Hu, B., Gao, T., Chen, Y., Gao, X., 2019. Mannan oligosaccharides trigger multiple defence responses in rice and tobacco as a novel danger-associated molecular pattern. Mol. Plant Pathol 20, 1067–1079.